Genomic regulatory landscape underlying the antiviral response of Atlantic salmon

Shahmir Naseer[1], Thomas Clark[1], Bertrand Collet[2], Pooran Dewari[3], Damir Baranašić[4], Daniel J. Macqueen[3], Pierre Boudinot[2*] and Samuel A. M. Martin[1*]

[1]Scottish Fish Immunology Research Centre, School of Biological Sciences, University of Aberdeen, Aberdeen, UK

[2]Université Paris-Saclay, INRAE, UVSQ, VIM, Jouy-en-Josas, France

[3] The Roslin Institute and Royal (Dick) School of Veterinary Studies, University of Edinburgh, Easter Bush Campus, UK

[4]Ruđer Bošković Institute, Laboratory for Computational Biology and Translational Medicine, Bijenička, Zagreb, Croatia

Corresponding authors: Samuel A.M. Martin sam.martin@abdn.ac.uk and Pierre Boudinot pierre.boudinot@inrae.fr

Abstract

All jawed vertebrates have a highly coordinated innate immune response to viral infections driven by a core set of interferon responsive genes (ISGs), but interspecies variation remains substantial. In this study, we examined the genome-wide regulatory basis for antiviral gene expression responses in Atlantic salmon (*Salmo salar*), representing a teleost family that underwent a whole genome duplication (WGD) event ~100 Mya. We stimulate fish systemically with polyinosinic:polycytidylic acid (poly I:C), a synthetic viral mimic, and profile transcriptomic and epigenomic responses in the primary haematopoietic and lymphoid tissue. We used ATAC-seq and ChIP-seq (H3K27ac and H3K27me3), combined with mRNA-seq, to comprehensively examine modifications in gene regulation following stimulation. We identified a set of 197 ISGs with regulatory elements showing increased chromatin accessibility and H3K27ac signal in concert with increased gene expression in response to poly I:C. Fifty-four of these genes were conserved ISGs in rainbow trout, zebrafish, and human. Our analysis provides evidence for conserved transcription factors (TFs) driving the interferon response by binding ISG promoters, including IRF8, IRF9, STAT1, and STAT2. Regulatory elements within differentially expressed genes were enriched for predicted binding sites for STAT6, PRDM1, IRF6, JDP2, NR2E1, and BCL6, suggesting a central role for these TFs in the antiviral response. Finally, we demonstrate paralogue-specific enrichment of interferon-stimulated response element (ISRE) motifs in poly I:C activated promoters of ISGs retained as duplicates from the salmonid WGD. Overall, this study provides novel insights into the genomic regulatory landscape underlying antiviral immunity in a farmed fish with a complex genome.

Introduction

The innate immune response to viral infection, which is mainly based on the type I interferon (type I IFN) pathway is crucial to both disease progression and the outcome of infection. Type I IFNs are present in all gnathostomes, and play a pivotal role in inducing an antiviral

state in host responding cells by the induction of IFN stimulated genes (ISGs) (Schoggins, 2019).

This antiviral response is triggered when viral pathogen-associated molecular patterns (PAMPs) bind to pattern recognition receptors (PRRs) such as toll-like receptors (TLR3, TLR7, TLR8) and RIG-I-like receptors (RLRs), activating downstream signalling cascades that induce transcription of type I interferons (IFNs) and antiviral effectors (Thompson *et al*., 2011). In mammals, teleost fish and other vertebrate species this response is regulated at multiple levels, including complex transcriptional feedback loops and chromatin-mediated control of key antiviral genes (Ivashkiv and Donlin, 2014; Castro *et al*., 2014; Dehler et al., 2019). Epigenetic modifications such as histone acetylation and methylation contribute to this regulation by altering DNA accessibility at enhancers and promoters (Mostafavi *et al*., 2016; Kan *et al*., 2022). Transposase-accessible chromatin with sequencing (ATAC-seq) and chromatin immunoprecipitation and sequencing (ChIP-seq) are widely used to map open chromatin and histone modifications across the genome, enabling the identification of putative regulatory elements. While these assays are powerful, they have limitations, including the potential for false positives (regions that are accessible but not functionally active) and false negatives (context-dependent enhancers that may be missed in bulk analysis). Nonetheless, ATAC-seq and ChIP-seq have proven effective in both mammalian and teleost systems for revealing the epigenomic architecture of immune tissues and mapping regulatory elements associated with interferon responses (Cooper *et al*., 2024; Harvey *et al*., 2024; Tan *et al*., 2025).

The induction of type I IFN typically involves an initial detection and recognition of viral RNA by cytoplasmic RNA helicases like RIG-I and Melanoma Differentiation-Associated protein 5 (MDA5) or TLRs (TLR3, TLR7/8) (Matsumoto *et al*., 2003; Liu, 2005). In human or mouse, this leads to the production and secretion of IFNα and β, which then bind to their cognate receptors, interferon alpha/beta receptor 1 (IFNAR1) and 2 (IFNAR2) present on the surface of target cells. Activation of these receptors induces a signalling cascade leading to the

phosphorylation of the Janus kinases Tyk2 and JAK1, as well as the “signal transducers and activators of transcription” STAT1 and STAT2 (Platanias, 2005). These phosphorylated STAT1 and STAT2 molecules then bind with a third subunit, interferon regulatory factor 9 (IRF9), to form the IFN stimulated gene factor 3 (ISGF3) complex (Platanitis *et al* 2019). After translocation to the cell’s nucleus, ISGF3 binds to interferon-stimulated response elements (ISRE) in the promotors of ISGs, rapidly activating diverse genes with effector and regulatory immune function (Platanias, 2005; Ivashkiv and Donlin, 2014). The binding of ISGF3 to ISREs is essential for the induction of ISGs and for establishing an antiviral cellular state (Wang *et al.*, 2017). Multiple type I IFNs are present in and orchestrate antiviral innate responses teleost fish (Langevin *et al*., 2019). The ISG repertoire is more complex than in mammals, with additional gene family member paralogues being retained following whole genome duplication events (Collet *et al*., 2009; Skjesol *et al*., 2010; Briolat *et al*., 2014; Macqueen *et al*., 2014; Levraud *et al*., 2019; Gan *et al*., 2020; Clark *et al*., 2023). In addition to the presence of mammalian orthologs and their paralogous genes resulting from whole genome duplication, several gene families involved in antiviral immunity such as GCRV-induced gene 1 (gig1), RNA-dependent protein kinase (pkr/pkz), and specific TRIM gene subsets such as finTRIMs are unique to teleost fish. These teleost-specific ISGs likely evolved during lineage-specific expansions and are thought to play important roles in shaping fish-specific interferon responses or could have been lost in the lineages leading to tetrapods (An *et al*., 2025).

While the teleost IFN response has been extensively analysed at the transcriptomic level (e.g. Martin *et al.*, 2007; Zou and Secombes, 2011; Briolat *et al.*, 2014; Levraud *et al.*, 2019; Clark *et al.*, 2023) and functionality of ISREs has been proposed (Boudinot *et al*., 2001; Collet and Secombes, 2001; Castro *et al.*, 2008, 2010), the regulatory basis of the IFN system, and more generally antiviral transcriptional responses, remains poorly understood. To tackle this knowledge gap, we investigated the genomic regulatory mechanisms driving

core ISG expression responses in the head kidney of Atlantic salmon (*Salmo salar*), a globally important aquaculture species.

We hypothesised that: (i) gene regulation in response to poly I:C stimulation involves coordinated changes in chromatin accessibility and histone modifications, similar to mechanisms described in higher vertebrates; (ii) regulatory divergence between paralogous genes contributes to their differential expression during the antiviral response; and (iii) expanded or salmonid-specific gene families exhibit distinct regulatory signatures that reflect their functional roles in immunity.

To test these hypotheses, we integrated ATAC-seq, ChIP-seq and RNA-seq datasets following *in vivo* stimulation with the viral dsRNA mimic poly I:C. ChIP-seq was performed using the histone marks H3K27ac and H3K27me3. H3K27ac is an activating mark associated with open chromatin and transcriptionally active genes, marking promoter and enhancer regions (Wang *et al.*, 2008; Creyghton *et al.*, 2010). In contrast, H3K27me3 is a repressive mark associated with polycomb-mediated transcriptional repression and gene silencing (Bernstein *et al.*, 2006; Barski *et al.*, 2007), typically associated with regulatory regions of inactive genes. As salmonid genomes are characterised by two rounds of whole genome duplication (WGD) (Lien *et al.*, 2016; Robertson *et al.*, 2017), leading to the expansion and functional diversification of many gene sets compared to mammals (including ISGs: Clark *et al*., 2023), we further compared the regulation of ISG paralogues to seek evidence for changes in regulation or function. Our findings advance understanding of immune function, providing insights into the evolution of teleost fish paralogous ISGs at the regulatory level, while demonstrating functional conservation of key antiviral regulatory elements across vertebrates.

Results

In this study we examine the modulation of gene expression, chromatin accessibility and histone modifications in Atlantic salmon following stimulation using poly I:C, a mimic of

infection with an RNA virus. A major transcriptomic response was elicited driving the upregulation of a core set of ISGs (Clark *et al*., 2023), in this report we use the term ISGs to include all genes inducible within the interferon response including those that are directly upregulated by poly I:C stimulation. The aim of the current study is to elucidate epigenomic changes in chromatin state following this stimulation and shed light on regulatory elements and TFBSs influencing antiviral transcriptional responses in a complex teleost genome.

Genomic sequencing data and sample metadata

Thirty-eight datasets were generated, comprising ATAC-seq (12 datasets: n=6 Poly I:C, n=6 PBS control) and ChIP-seq (12 datasets per histone mark: n=6 Poly I:C, n=6 PBS; along with 2 input controls). For H3K27ac, one PBS sample was excluded from the analysis post-sequencing, while for H3K27me3, one sample each for PBS and Poly I:C were excluded. Full details regarding samples and sequence data are provided in Supplementary Table 1. ATAC-seq provides genome-wide identification of open chromatin regions, and with six control and six poly I:C stimulated fish, offers in-depth data to study regulatory elements, TFBS, and changes in chromatin accessibility. ChIP-seq was performed using two histone modifications: H3K27ac and H3K27me3. Promoters and enhancers were defined based on chromatin accessibility, histone modifications, and ChromHMM annotations. Regions classified as putative promoters were those overlapping transcription start sites (TSS) with ATAC-seq consensus peaks and H3K27ac enrichment, indicative of active regulatory activity. Specifically, candidate enhancers were identified as intergenic or intronic regions that exhibited both ATAC-seq accessibility and H3K27ac modification, suggesting distal regulatory elements. Peaks marked predominantly by H3K27me3 were classified as polycomb-repressed regions, reflecting transcriptionally silent chromatin states. These ChromHMM annotated enhancers and promoters, defined through the integration of ATAC-seq and H3K27ac, were subsequently used for downstream TFBS analysis, allowing the identification of key regulatory motifs involved in the antiviral response.

To further characterise the genomic distribution of ATAC-seq and H3K27ac peaks, we annotated consensus peaks relative to gene features and transcription start sites (TSS). The majority of peaks in both ATAC-seq and H3K27ac datasets were associated with genes (Figure 1A and 1B) and enriched in promoter-proximal and enhancer regions, with a high density observed within 50 kb of the TSS (Figure 1C and 1D). This confirms the utility of these datasets for identifying active regulatory elements in the Atlantic salmon genome.

Immune stimulation remodels chromatin accessibility and histone modifications in Atlantic salmon head kidney

Poly I:C stimulation led to widespread changes in chromatin accessibility, with an approximately 25% increase in ATAC-seq peaks detected in treated fish (53,102 ± 6,142) compared to PBS controls (39,869 ± 11,858). These accessible regions were distributed across promoter-TSS (10%), exonic (13%), intronic (45%), and intergenic (26%) features of the genome (Supplementary Figure 2A). To illustrate the data quality and consistency, genome browser tracks at the housekeeping gene elf1a showed well-defined cis-regulatory peaks in both conditions, matching the expected expression patterns (Figure 2A and B).

Differential analysis identified 613 regions (250 promoters, 363 enhancers) with increased accessibility and 48 regions (6 promoters, 42 enhancers) with reduced accessibility after poly I:C stimulation (fold change > 2, padj < 0.05) (Figure 2E; Supplementary Table 2). Functional enrichment of the regions with increased accessibility, performed using rGREAT, highlighted pathways central to antiviral immunity, including “regulation of cytokine-mediated signalling,” “interferon-mediated signalling,” and “type I interferon response” (Figure 2C; Supplementary Table 3A). Several terms related to JAK-STAT signalling and host-virus interactions were also among the top enriched categories.

Chromatin immunoprecipitation profiling of H3K27ac and H3K27me3 marks further revealed distinct patterns of histone modification following immune stimulation. Stimulated fish showed an average of 72,490 (±21,211) H3K27ac and 68,873 (±16,608) H3K27me3 peaks, compared to 78,816 (±31,106) and 48,221 (±26,905) in PBS controls. Analysis of differential abundance identified 1,539 regions enriched for H3K27ac (528 promoters, 1,011 enhancers) and 794 regions enriched for H3K27me3 (124 promoters, 670 enhancers), while a comparable number of regions were lost for each respective mark in response to stimulation (Figure 2F and G; Supplementary Table 4). A small subset of loci (45) exhibited reciprocal regulation, gaining H3K27ac while losing H3K27me3, suggesting polycomb-mediated

repression was relieved to allow gene activation (Supplementary Figure 3C; Supplementary Table 5). In contrast, only 30 regions showed concurrent increases in both marks, supporting the notion that their regulation is largely independent in this context (Supplementary Figure 3A).

Gene set enrichment of regions gaining H3K27ac underscored their association with immune processes, including “interferon-mediated signalling,” “cellular response to type I interferon,” “response to virus,” and pathways involved in epithelial and endothelial cell migration (Figure 2D; Supplementary 3B). Comparison of the enriched biological processes revealed that 8 out of the top 15 GO terms identified in ATAC-seq peaks were also significantly enriched among regions gaining H3K27ac. These shared terms included hallmark antiviral processes such as “interferon-mediated signalling pathway” and “response to type I interferon” and “regulation of receptor signalling pathway via JAK-STAT”, reflecting coordinated chromatin accessibility and histone acetylation at critical immune loci. These findings demonstrate a coordinated regulatory response to poly I:C, involving both chromatin accessibility and activating histone modifications at key antiviral loci.

Multiomics identifies epigenomic changes associated to the induction of core ISGs

To uncover the regulatory mechanisms underlying the transcriptome response induced by poly I:C, we integrated data from RNA-seq, ATAC-seq, and ChIP-seq for the active histone mark H3K27ac and repressive histone mark H3K27me3. For this analysis, we defined 3,541 genes associated with changes across all four assays, split into five subsets with distinct regulatory profiles (Figure 3A). Of interest we find different groups of genes that are activated at different levels, these are: (1) Core genes (197 genes; set 1) were defined by significant concurrent increases in ATAC-seq chromatin accessibility, H3K27ac signal, and mRNA expression following poly I:C stimulation. The presence of both open chromatin regions and H3K27 acetylation close to these genes suggests that these regions function as candidate active enhancers and promoters, driving transcriptional activation in response to stimulation (Figure 3B). The second gene set (1,348 genes; set 2) exhibited significant increases in chromatin accessibility and H3K27ac signal without corresponding transcriptional upregulation. These regions likely represent candidate active enhancers and

promoters that are primed for activation but may require additional regulatory inputs for transcriptional induction (Figure 3C), (3) genes where mRNA expression is increased but lacking changes in chromatin accessibility (1,008 genes; set 3) (Figure 3D), (4) genes showing increased mRNA expression and chromatin openness, but lacking changes in H3K27ac signal (52 genes; set 4) (Figure 3E) and (5) genes with significant increases in H3K27ac signals alongside transcript-level upregulation (173 genes; set 5) (Figure 3F; Supplementary Table 6). Canonical antiviral genes were mainly enriched in Set 1, which exhibited coordinated increases in gene expression, chromatin accessibility, and H3K27ac. This group included key effectors such as *TRIM25, RSAD2, IRF7, MX1*, and *IFI44*. Additional antiviral genes, such as *STAT1* and *IRF8*, were found in Set 3 (RNA-seq only). Few antiviral genes were detected in Sets 2, 4, or 5, underscoring Set 1 as the principal group reflecting multi-layered antiviral gene regulation.

The core 197 genes (set 1 above) displayed increases in chromatin openness and H3K27ac signal alongside significant transcript upregulation, underscoring their tight regulatory coordination. Functional enrichment for GO terms revealed these genes are primarily involved in early innate immune responses, with significant enrichment for terms such as *"response to virus"*, *"innate immune response"*, and *"protein ubiquitination"* (Figure 3B). Importantly, further analysis of this subset revealed that 54 (27%) of the 197 genes overlapped with the core set of Atlantic salmon ISG induced in vivo that are conserved between salmon and human (154 genes) (Clark *et al*., 2023) (Supplementary Figure 4; Table 1). This is significantly higher (two-tailed Fisher's exact test, $p < 0.0001$) than the conserved ISG proportion among all poly I:C induced genes (154 out of 1,446 transcriptionally induced genes i.e. 11%), this evolutionary conservation underscores the central importance of these genes in antiviral immunity.

A subset of 1,348 genes (set 2 above) showed significant increases in chromatin accessibility and H3K27ac signal without corresponding changes in transcript levels. To further investigate this finding, we analysed the genomic context of the associated peaks.

Many peaks were located in intergenic or intronic regions, indicative of putative enhancers. As enhancers often regulate distal genes rather than the closest annotated gene, this could explain the absence of detectable changes in RNA levels for nearby loci. For peaks associated with promoters, the increased chromatin accessibility and H3K27ac signal may reflect transcriptional activation that is not captured in total RNA-seq data. This could occur if small transcriptional changes are masked by the stability and abundance of pre-existing transcripts in the cytoplasm. The corresponding gene set did not exhibit enrichment for antiviral or interferon response pathways, suggesting potential involvement in alternative biological processes (Figure 3C).

Third, we identified a subset of genes (set 3 above) that were differentially expressed in response to poly I:C but did not exhibit changes in chromatin accessibility or histone mark modifications. These genes were enriched for GO terms such as "*cellular response to virus*", "*positive regulation of NF-kappaB transcription factor activity*", "*response to lipopolysaccharide*", "*cellular response to type II interferon*", and "*inflammatory response*" (Figure 3D), highlighting their pivotal role in the antiviral response.

Fourth, we identified a set of 52 genes (set 4 above) that exhibited significant changes in chromatin accessibility and transcript levels, without corresponding alterations in H3K27ac marks. GO term enrichment for these genes included "*T-helper 2 cell differentiation*" and "*response to virus*" (Figure 3E). The lack of H3K27ac changes suggests that these genes might be regulated through distal enhancers, changes in chromatin topology, or mechanisms unrelated to histone acetylation.

Fifth, a distinct set of 173 genes showed significant increases in H3K27ac signals alongside transcript-level upregulation, but no ATAC-seq signal. These genes were enriched for GO terms such as "*defence response to virus*", "*innate immune response*", "*protein ubiquitination*", and "*signal transduction*" (Figure 3F), reflecting their active involvement in the antiviral response. The concurrent increase in H3K27ac and gene expression strongly

supports their role as actively transcribed loci, with acetylation marking a key feature of them in response to poly I:C stimulation.

Finally, a subset of 747 genes was exclusively associated with increase in repressive histone mark H3K27me3, which is typically linked to transcriptional silencing through repressive polycomb complexes, with known roles in regulating immune responses (Bosselut, 2016). However, GO analysis did not reveal any significantly enriched terms for this subset, indicating a lack of strong functional enrichment for these genes.

A key ISRE motif, IRF8 drives the antiviral gene regulatory network

To further investigate regulatory mechanisms driving the antiviral response, we focussed on the core set of 197 genes identified above showing coordinated changes in expression, chromatin accessibility and H3K27ac signal. TFBS enrichment analysis was performed on the peaks or regions corresponding to those 197 genes containing both enhancers and promoters, which revealed nine enriched TFBS (Figure 4A). The most enriched TFBS was interferon regulatory factor 8 (IRF8), a highly characterised binding site utilised during interferon responses (Mancino *et al*., 2015). IRF8 binding site was identified in the regulatory regions of 37 of the 197 genes (18.8%), and all these genes were also highly significantly upregulated at the mRNA level, supporting the functional relevance of IRF8 motif enrichment in the antiviral response (Table 2). The IRF8 binding site corresponds to the ISRE, a motif that has core elements of nnGAAAnnGAAAnn (Figure 4B) shared with many other ISRE elements found in or near interferon responsive genes (Tamura *et al*., 2015). This ISG subset includes key antiviral effectors such as *MX*, an IFN-inducible dynamin-like large GTPases that is well characterised to mediate antiviral activities; a TRIM ubiquitin ligase involved in viral neutralization; *MEFV*, a key regulator of innate immunity; and *PARP14*, a poly(ADP-ribose) polymerase involved in transcriptional activation of ISGs (Haller *et al*., 2007; Caprara *et al*., 2018; Koepke *et al*., 2021). The TFBS motif for IRF8-binding motifs (Figure 4B) confirms the functional conservation of the ISRE sequence, consistent with its binding preferences and regulatory function in ISGs. These findings are consistent with the

earlier observation of GO term enrichment for the 197 genes (Figure 3B), which were associated with processes such as *"response to virus*" and "*innate immune response*". The prevalence of IRF8 motifs within these genes further supports this TF's role as a critical transcription factor driving interferon-stimulated regulatory networks during poly I:C stimulation.

Chromatin state dynamics and TFBS using whole ATAC-seq and ChIP-seq data sets

To investigate the chromatin landscape underlying the antiviral immune response to poly I:C, we applied ChromHMM modelling to the ATAC-seq, H3K27ac, and H3K27me3 datasets. This integrative analysis identified five distinct chromatin states, annotated following the framework established by Ernst and Kellis (2017) (Figure 5A, B and C). These chromatin states were classified as follows: (1) ATAC Islands: regions characterized by high chromatin accessibility, indicative of active regulatory activity lacking H3K27ac and H3K27me3 and the presence of potential enhancer or promoter elements. (2) Quiescent/Low Regions: Areas with minimal chromatin accessibility and low regulatory activity, suggesting these regions are largely inactive under the conditions tested. (3) Repressed States: Regions dominated by H3K27me3 with low ATAC-seq signal, indicative of transcriptional silencing mediated by polycomb repression. (4) Poised Enhancer States: Regions marked by H3K27me3 (repressive mark) alongside H3K4me1, indicative of enhancers that are primed but not yet active. These regions may transition to an active state upon specific stimuli through the loss of H3K27me3 and the acquisition of H3K27ac, which marks active enhancers (Barral and Déjardin, 2023). (5) Active Regulatory Elements (Enhancers/Promoters): Regions displaying strong ATAC-seq and H3K27ac signals, reflecting robust regulatory activity and heightened chromatin accessibility at enhancers and promoters. ChromHMM analysis revealed that chromatin state 5, corresponding to active enhancers and promoters (enriched for ATAC-seq and H3K27ac signals), was more prevalent in poly I:C stimulated samples compared to PBS controls (Figure 5B and C), consistent with increased activation of regulatory regions during the antiviral response. These findings provide a high-resolution view of chromatin state

dynamics, illustrating the diversity of regulatory landscapes and their functional relevance in response to poly I:C stimulation.

To identify transcription factors potentially regulating these active regions, consensus open chromatin regions representing ChromHMM state 5 (active regulatory elements) were analysed for TFBS enrichment (Figure 5D). Sixteen TFBSs were either significantly enriched or under-represented in poly I:C. Seven TFBSs were uniquely enriched in the poly I:C stimulated group, including STAT6, IRF9, PRDM1, IRF6, JDP2, NR2E1, and BCL6. These transcription factors play central roles in antiviral immunity and immune system regulation. The presence of STAT6 (Li *et al*., 2016), IRF9 and IRF6 demonstrates a set of key TFBS for interferon responsive genes, with IRF9 sharing a binding site highly similar with IRF8 described earlier.

ISREs reside within regulatory elements driving the antiviral response

The enrichment of TFBSs for conserved vertebrate interferon regulators including IRF3, IRF7, IRF8, IRF9 and STAT2, implies the activation of ISGs through the ISRE pathway. In this context, our focus was directed towards investigating the response induced by primary viral recognition facilitated by the RIG-I pathway, which play a central role in initiating the interferon response and establishment of an antiviral cellular state (Figure 6A). Specifically examining the RIG-I pathway, we observed upregulation of *rig-i*, *mda5*, *irf3*, and *irf7* at the mRNA level, with a concurrent significant increase in associated peaks in ATAC-seq and H3K27ac datasets. However, while *mavs* was expressed, but as previously demonstrated this gene was not induced by viral infection (Biacchesi *et al*., 2009) (Figure 6B). Notably, *rig-i* and *mda5* displayed reduced promoter H3K27me3 (repressive mark) signal in response to poly I:C, suggesting their activation rather than suppression during this immune antiviral response. Turning to the JAK-STAT pathway, we observed significant induction of *stat1*, *stat2*, and *irf9* mRNAs, accompanied by a notable increase in promoter openness and H3K27ac signal, and a visible decrease in promoter H3K27me3 signal for *stat2* and *irf9*. These results clearly demonstrate combined chromatin activation and expression

upregulation of the major signalling transcription factor genes involved in interferon and antiviral responses.

We further sought to identify ISREs within genes associated with the RIG-I and JAK-STAT pathways. Our criteria for enrichment included the presence of ISREs within promoter regions exhibiting increased accessibility and/or concurrent H3K27ac activity in response to poly I:C. Notably, *rig1* and *mda5* share the ISRE consensus sequences *TTTCGGTTTC* and *TTTCGTTTC* in their proximal promoters (Figure 6C), while *irf7* and *stat1* share *TTTCACTTC* as their exclusive ISRE (Figure 6C and D). *irf3* featured a single ISRE, *GAAAACGAAA*, whereas *stat2* and *irf9* harbour two ISREs within their proximal promoters (Figure 6D).

We also searched for ISREs in additional key ISGs that were differentially expressed and showed increased chromatin openness and H3K27ac activity upon poly I:C simulation. We focused on five genes captured in multiple enriched GO terms for antiviral activity with strong mRNA upregulation by poly I:C: *mx*, *rsad2*, *tapbp*, *isg15*, and *cd9*. ISREs were enriched in the proximal promoter of these genes, including two for *mx* (*GAAATGAAA* and *TTTCGATTTC*), two for *cd9* (*TTTCATTTC* and *TTTCTTTTC*), three for *rsad2* (*GAAACGAAA, TTTCGTTTTC* and *TTTCATTTTC*), three for *tapbp* (*GAAAGGAAA, TTTCACTTTC* and *TTTCATTTTT*), and one for *isg15* (*GAAACCGAAA*) (Figure 7A and B). The peaks associated with ISRE motifs in the H3K27me3 dataset were either significantly lower or remained unchanged following poly I:C stimulation, suggesting that these regions are repressed and do not undergo activation in response to the stimulus (Figure 7B).

ISRE enrichment is paralogue specific

Salmonid fish have expanded gene families with paralogues retained from both ancestral WGDs and tandem gene duplications. Our previous work has demonstrated differential expression in response to poly I:C among paralogous ISGs (Clark *et al*., 2023). To further

368 explore the regulation of these paralogues, we conducted paralogue-specific ISRE motif
369 analysis for key ISGs, including *mx*, *rsad2*, *irf9*, *irf7*, *dhx58*, *stat1*, and *cd9* (Supplementary
370 Figure 5).

371 Within the *mx* gene family, seven paralogues were identified, with four showing highly
372 induced gene expression (ENSSSAG00000077530, ENSSSAG00000117576,
373 ENSSSAG00000096170, and ENSSSAG00000051905) (Supplementary Figure 5A).
374 Notably, only the most upregulated *mx* paralogue (ENSSSAG00000077530) possessed
375 ISREs in its putative promoter (*GAAATGAAA* and *TTTCGATTTC*). Four of these mx
376 paralogues are tandem repeats located on Chromosome 25.

377 The *rsad2* gene family comprised four paralogues, three of which were highly upregulated by
378 poly I:C (ENSSSAG00000048046, ENSSSAG00000108937, and ENSSSAG00000108840),
379 each harbouring two or three ISRE motifs with *GAAACGAAA* shared (Supplementary Figure
380 5B). Three *rsad2* genes were found as tandem repeats on Chromosome 9, two with
381 identified ISREs (ENSSSAG00000108840 and ENSSSAG00000108937) (Supplementary
382 Figure 5B).

383 *irf9* and *irf7* have two and three paralogues, respectively. Only one *irf9* paralogue
384 (ENSSSAG00000080439) exhibited ISRE motifs (*AAAACCGAAA* and *AAAAACGAAA*) in
385 regulatory elements activated by poly I:C (Supplementary Figure 5C). For *irf7* one paralogue
386 (ENSSSAG00000076373) contained the ISRE *TTTCACTTTC* in activated regulatory
387 elements (Supplementary Figure 5D). A second *irf7* paralogue (ENSSSAG00000066279)
388 displayed open chromatin at the promoter, though chromatin accessibility was not
389 significantly different between stimulated and unstimulated fish, suggesting alternative
390 regulatory mechanisms.

391 The core viral receptor gene family *rig-I* has three paralogues (ENSSSAG00000037858,
392 ENSSSAG00000003156, and ENSSSAG00000119673), all showing the presence of ISREs
393 within regulatory elements activated by poly I:C stimulation (Supplementary Figure 5E).

In the *stat1* family, three out of five paralogues harboured ISREs in upstream regulatory regions activated by poly I:C stimulation (Supplementary Figure 5F). One copy (ENSSSAG00000056374) had open chromatin without any ISRE, and another (ENSSSAG00000102446) did not display open chromatin in the promoter.

The *cd9* family comprised eight paralogues, with only ENSSSAG00000059637 exhibiting ISRE regions (*TTTCATTTC* and *TTTCTTTTC*) in the proximal promoter, which was associated with the strongest mRNA expression and upregulation by poly I:C (Supplementary Figure 5G). Four of these paralogues were identified as contigs, representing highly duplicated sequences not assignable to specific chromosomes due to their repetitive nature.

Our paralogue specific ISRE motif analysis unveils distinct regulatory patterns and functional implications within the innate immune response, shedding light on the intricate dynamics of gene paralogues in antiviral defence mechanisms.

Discussion

The immune response to viral infections is a fundamental aspect of host defence mechanisms conserved across vertebrates. In this study, we combined RNA-seq, ATAC-seq and ChIP-seq to investigate the regulatory landscape underlying the antiviral response in Atlantic salmon following poly I:C stimulation, a mimic of double-stranded RNA viruses. Our aim was to elucidate the interplay between gene expression, chromatin accessibility, and histone modifications during the early stages of the immune response.

Our analysis revealed significant alterations in both the transcriptome and ‘regulome’ in response to poly I:C stimulation. Notably, these changes were observed in a subset of conversed ISGs, which play an important role in antiviral defence in all vertebrates. ATAC-seq provided valuable insights into chromatin accessibility alterations during the antiviral response, revealing hundreds of regions exhibiting significant changes following poly I:C

stimulation. The functional significance of these open chromatin regions was supported by enrichment of Gene Ontology terms related to viral response for the nearby genes they presumably regulate. H3K27ac and H3K27me3 histone modifications are key players in gene regulation (Creyghton *et al*., 2010; Barski *et al.*, 2007). Our study revealed a significant increase in H3K27ac activity in 1,539 genomic regions, indicative of gene activation. Conversely, the upregulation of H3K27me3 in 795 regions suggests transcriptional suppression and the formation of repressive chromatin structures. Only 30 genomic regions exhibited concurrent changes in both H3K27ac and H3K27me3. While these marks are typically considered mutually exclusive, their detection within the same genomic regions is likely to reflect cell-type heterogeneity, where the same regulatory element is repressed (H3K27me3) in some cell populations while being active (H3K27ac) in others. This may indicate differential regulatory states across distinct cell subsets rather than a true bivalent chromatin state (Barral and Déjardin, 2023). These regions may play critical roles in maintaining essential cellular processes or fine-tuning immune response regulation, potentially through mechanisms involving chromatin remodelling and transcription factor recruitment. Collectively, the integration of ATAC-seq and ChIP-seq data provides comprehensive insights into regulatory changes in Atlantic salmon in response to viral stimulation.

We find 3,541 genes that show differential expression following poly I:C stimulation, which together are consistent with different layers of regulatory changes representing different functional groups of genes. The core set of 197 genes that are transcriptionally upregulated and also have significant increased open chromatin and increased presence of activating H3K27ac is enriched in ISGs conserved among vertebrates (Clark *et al*., 2023). Of interest there were also genes that showed chromatin remodelling, with no associated significant change in gene expression. These genes may represent a group of loci with distinct temporal regulation, potentially primed for expression either before or after the single time point analysed in our study. For instance, genes that exhibited changes in chromatin

accessibility and gene expression without accompanying H3K27ac modifications, suggest the involvement of distal enhancers or alternative chromatin dynamics such as topologically associating domains (TADs) influencing their regulation (Tena and Pereira, 2021). The genes that are defined as having chromatin openness and increased expression have very clear interferon associated functionality, which could reflect different activation modes of histone modification (H3K4me3 and H3K4me1), as in our study we examined a single activating histone mark (Murphy *et al*., 2024). The large number of genes that are transcriptionally upregulated but lack significant changes in chromatin accessibility and histone acetylation (H3K27ac), exhibit a very clear role in the IFN response. These genes likely represent early response genes that are already in an accessible chromatin state, allowing for rapid transcriptional activation upon stimulation (Bahrami and Diablos, 2016). Alternatively, these genes may be regulated post-transcriptionally following poly I:C stimulation, a mechanism often observed in innate immune responses, which could involve mRNA stability, translation efficiency, or degradation pathways (Carpenter *et al*., 2014).

Recent single-cell transcriptomic studies have highlighted the remarkable cellular heterogeneity of Atlantic salmon immune cells, particularly in the head kidney (Andresen *et al*., 2024) and in the liver (Taylor *et al*., 2022). This diversity likely underlies the observed largely disconnected regulation of H3K27ac and H3K27me3 marks in response to poly I:C, as different immune cell subpopulations likely exhibit distinct patterns of chromatin remodelling at the same loci. Although a detailed, locus-by-locus inspection was beyond the scope of this study, our findings are consistent with the idea that cellular heterogeneity shapes the chromatin and transcriptional responses to antiviral stimulation. Incorporating such single-cell insights in future studies will be valuable for resolving how specific cell types contribute to the epigenomic regulation of the interferon response in salmonid immunity.

ISREs are DNA sequence motifs responsible for the regulation of immune genes (Au *et al*., 1995), which serve as recognition sites for transcription factors integral to the interferon response pathway (Ivashkiv and Donlin, 2014). Our analysis identified a notable enrichment

of TFBSs specific to IRF8, IRF9, STAT1, and STAT2 in response to poly I:C stimulation. These transcription factors are well-documented to bind to ISREs (Au-Yeung *et al*., 2013; Platanitis *et al*., 2019), underlining the significance of transcription factor-mediated regulatory mechanisms governing the antiviral immune response in Atlantic salmon. IRF8 exhibited the highest level of enrichment in those genes which were identified across RNA-seq, ATAC-seq, and H3K27ac datasets. These genes included key antiviral effectors, such as *TRIM21, MEFV*, and *PARP14*, which are involved in protein ubiquitination, immune modulation, and transcriptional activation of ISGs. IRF8, a transcription factor that binds to ISREs to regulate antiviral gene expression, is critical for immune responses across vertebrates. In humans and mice, IRF8 is crucial for the development and function of dendritic cells and macrophages, which are key players in antiviral defence and type I interferon production (Hambleton *et al*., 2011; Laricchia-Robbio *et al*., 2005). Studies on IRF8-deficient mice have demonstrated increased susceptibility to viral infections, linked to compromised dendritic cell populations and disrupted immune signalling pathways (Becker *et al*., 2012; Moorman *et al*., 2022). These findings, combined with the strong enrichment of IRF8 motifs in our dataset, highlight its evolutionary conservation and central role in orchestrating the antiviral immune response in Atlantic salmon.

Moreover, these transcription factors are known regulators of immune response genes during viral infections (Ivashkiv and Donlin, 2014). Our analysis demonstrates that ISRE-containing genomic regions undergo dynamic histone modifications during antiviral signalling, indicating their functional relevance in gene regulation. This study also expands upon previous research on ISREs in salmonids, focusing on gene families such as *mx, rsad2, stat1, stat2,* and *cd9* which were previously examined primarily at the expression level (Collet, 2004; Castro *et al*., 2008, 2010; Holland *et al*., 2008; Collins *et al*., 2014; Dehler *et al*., 2023). Earlier studies included *in silico* promoter analyses and reporter gene assays, but our integration of ATAC-seq and ChIP-seq datasets allows demarcation of genomic regions with putative functional involvement in the early antiviral response. However, further

experimental validation, such as knockout or knock-in studies targeting the identified regulatory elements, will be essential to confirm the molecular mechanisms underlying these observations.

The enrichment of TFBSs associated with IRF3 and IRF7 underscores their important role in the antiviral response of Atlantic salmon. The enrichment of TFBSs for PRDM1, IRF6, JDP2, NR2E1**,** and BCL6 highlights the diverse regulatory landscape governing the immune response in Atlantic salmon following poly I:C stimulation. PRDM1 (also known as BLIMP-1) is known for regulating type I IFN and differentiation of B cells in to plasma cells (Lin *et al.*, 1997), but also orchestrates plasma cell differentiation by extinguishing the mature B cell gene expression program (Shaffer *et al.*, 2002), while BCL6 is involved in B cell development in mammalian germinal centres (Tsai *et al.*, 2019). IRF6 further contributes to antiviral responses (Liang *et al.*, 2022). JDP2 has a core role in modulating inflammatory signalling pathways (Maruyama *et al.*, 2012) and NR2E1 is involved in neural development and has a crucial role in regulating the proliferation, differentiation, and maintenance of neural progenitor cells in various regions of the brain (Islam and Zhang, 2015). Despite our TFBS analysis relying on the JASPER database, primarily employing experimental data on mammalian transcription factors as the background, the enrichment of these TFBSs in response to poly I:C suggests their evolutionary conservation across vertebrate species, underscoring their relevance in understanding immune responses beyond Atlantic salmon.

Our analysis of enrichment in paralogue-specific ISRE motifs unveiled distinctive ISRE sequences exclusive to specific paralogues. Consequences of four rounds of whole-genome duplication (two in early vertebrates, one in the teleost ancestor, and one salmonid-specific) can be detected in the Atlantic salmon genome, a phenomenon well-documented in the literature (Lien *et al.*, 2016). This process has given rise to multiple paralogous genes that have evolved distinct regulation (e.g. Gillard *et al.*, 2021), as observed for many ISG families (Clark *et al.*, 2023). We identified paralogue-specific alterations in the chromatin accessibility of key ISGs, including genes such as *mx*, *rsad2*, *cd9*, *rig1*, *stat1*, *irf7*, and *irf9*. One outcome

following gene duplication and frequent subsequent silencing of the particular paralogue could relate to insertion of transposable elements into the regulatory regions of ISGs as was suggested for a decrease transcriptional activity across salmonid genomes where ohnologues showing decreased expression had great abundance of transposable elements (Gillard *et al*., 2021). In line with this genomic complexity, immune gene families exhibit heterogeneous distribution patterns, with some, such as finTRIMs, in gene groups dispersed across the genome while others, including MHC class I genes, form a few or a unique cluster on a specific location (Van der Aa *et al*., 2009; Lukacs *et al*., 2010). These findings underscore the importance of considering paralogue-specific responses in investigations of the interferon response in salmonids and other species with a history of WGDs.

This study has demonstrated the activation of putative regulatory elements initiating the antiviral response in a teleost fish by integrating transcriptomics and regulomics. We identified a conserved set of ISGs showing increased mRNA expression following antiviral stimulation, that is likely a product of transcriptional changes induced by remodelling of chromatin state and histone modifications. We further discovered the importance of paralogue-specific changes in key transcription factor binding sites, indicating that the regulatory control of key immune genes has been altered in the recent evolutionary history of salmonids. This work provides a new reference for functional analysis of immune response of Atlantic salmon / fish using transcriptomics, genomics and frames it in an evolutionary perspective.

Materials and Methods

Animal studies

Juvenile Atlantic salmon (~70g) of commercial origin were maintained in 250L freshwater tanks in the Zoology building aquarium at the University of Aberdeen (School of Biological Sciences). Water temperature was maintained at 14°C, and fish were fed a commercial

pellet diet. The water flow rate was approximately 1000L/h and photoperiod was 12:12 light:dark. All procedures described complied with the Animal (Scientific Procedures) Act of 1986 under the UK Home Office license PFF8CC5BE and were approved by the ethics committee at the University of Aberdeen, Scotland, United Kingdom.

Stimulation of fish with viral mimic

Poly I:C (Sigma, P1530) was diluted to 5 mg/mL in PBS, aliquoted and stored at -20 °C. Prior to being used for immune stimulation, poly I:C was heated to 55 °C for 15 minutes and then allowed to cool at room temperature for 20 minutes. Fish were anaesthetised using 2-phenoxyethanol (2.5 mL in 10 L water/ 0.0025 % v/v) and given an intraperitoneal injection of either PBS (1×, 0.1 mL) (n=6, controls) or poly I:C (500 µg in 0.1 mL, per fish) (n=6). 24 hours after stimulation, fish were euthanised by overexposure to 2-phenoxyethanol followed by destruction of the brain using a scalpel. Head kidney tissue was sampled – chosen for this study as the primary haematopoietic tissue in teleosts, rich in different leucocyte populations. For RNA-seq, samples were stored in RNAlater (Sigma) for 24 hrs at 4°C followed by long-term storage at -80 °C. For ATAC-seq and ChIP-seq, fresh head kidney tissue was placed in L15 media (Gibco) containing 2 % FBS (Labtech) and 0.02 % EDTA (Sigma) and placed on ice until processing. For each fish (n=6 per PBS and poly I:C injected groups) one RNA-seq, one ATAC-seq and two ChIP-seq libraries (H3K27ac and H3K27me3 histone marks; see later section) were constructed from the same head kidney sample to facilitate data integration (Supplementary Figure 1).

ATAC-seq library preparation

ATAC-seq library preparation was adapted from Buenrostro *et al.* (2015). Head kidney tissue (~20 mg) was placed into a 50 mL tube (tube 1) containing 20 mL extraction media (L15, 2 % FBS and 0.02 % EDTA, pH 8). The tissue was gently passed through a 100 µm nylon mesh (Starlab) and placed in a new 50 mL tube using a sterile pipette and spatula. Extraction media was continually applied to prevent cells from drying out and assist with their

transit through the mesh. This step disrupted the tissue, and cells were dissociated in the media. The final suspension of cells was made up to 20 mL in extraction media. An aliquot of 10 µL of these cells was mixed with trypan blue (Sigma) at a 1:5 ratio and counted using a haemocytometer. An aliquot of 75,000 cells for each sample was transferred in a 1.5 mL loBind Eppendorf tube for ATAC-seq library preparation, and the remaining cells were retained for ChIP-seq library generation as described in a later section.

Head kidney nuclei were isolated by pelleting the cells by centrifugation (500 g, 5 min, 4 ˚C). The supernatant was discarded carefully by aspiration to avoid cell loss. The cells were washed by resuspending then gentle pipetting in 1 mL PBS containing protease inhibitor cocktail (PIC) (Sigma). The cells were pelleted again (5 mins at 500 g at 4 ˚C), and the supernatant removed, to which 50 µL of cold ATAC-resuspension buffer L (ATAC-RSB-L) containing 0.1 % Tween-20, 0.1 % NP-40 and 0.01 % Digitonin (Promega) was added to the cell pellet, suspended by gently pipetting up and down three times. The ATAC-RSB cold buffer was made up of 1 M Tris pH 7.4 (Sigma), 5M NaCl (Sigma), 1M $MgCl_2$ (Sigma) and dH_2O. Cells were incubated on ice for 3 mins in cold ATAC-RSB-L to lyse the cells and release intact nuclei. Immediately after 3 mins, 1 mL of ATAC-RSB-W (ATAC-RSB-W contains ATAC-RSB and 10% Tween-20) with 0.1 % Tween-20 was added to the lysed cells. The tube was inverted three times and then centrifuged for 10 mins at 800 g at 4 ˚C to pellet the nuclei, before the supernatant was aspirated carefully to avoid losing the pellet.

The remaining ATAC-seq library preparation steps, such as transposase reaction, clean-up using MinElute PCR purification, library amplification and library clean-up, were performed according to Buenrostro *et al.* (2015).

ChIP-seq library preparation

ChIP-seq libraries were generated using the ChIPmentation Kit for Histones (Diagenode: Cat. No. C010110009). After tissue disruption and dissociation of cells in the extraction media, as described above for ATAC-seq, 2 $\times 10^6$ cells were transferred into a 1.5 mL tube

and pelleted for 10 mins at 800 g at 4 ˚C before the supernatant was carefully removed. Next, 1 mL of formaldehyde solution 1 % (Sigma) was added, and the pellet was then resuspended by pipetting up and down and incubated under constant rotation at room temperature for 5 mins to crosslink the DNA and proteins. The reaction was quenched by the addition of 125 µL of 1 M glycine (0.125 M final) and incubated for 10 mins at room temperature under constant rotation. The crosslinked cells were centrifuged for 5 mins at 1,000 g at 4 ˚C, and the supernatant removed. Next, cells were resuspended in 1 mL of PBS with PIC by pipetting and centrifuged for 5 mins at 1,000 g at 4 °C, before the supernatant was removed and the cell pellet was stored at -80 °C.

Sonication using a Bioruptor Pico device (Diagenode) was optimised at 20 cycles and 30 sec/30 sec on/off to disrupt the cells and shear the DNA. The sonicated chromatin was processed using the MinElute PCR purification kit (Qiagen). 20 µL sonicated chromatin was added to 180 µL elution buffer along with 2 µL of RNase A (100 mg/mL) and incubated for 10 mins at 37 °C. 5 µL Proteinase K (20mg/mL) was added before further incubation for 1 hour at 68 °C under constant rotation. DNA purification was performed using the MinElute PCR purification kit (Qiagen). DNA was then quantified using NanoDrop (One/One^{c} Microvolume UV-Vis Spectrophotometer, ThermoFisher Scientific) and assessed by Tapestation (4200) (Agilent Technologies) with a high-sensitivity DNA kit to determine DNA fragment size. A fragment size range of 100-700 bp was achieved for all downstream ChIP-seq library preparations. The remaining steps followed Diagenode's instructions for the ChIPmentation Kit. The two antibodies used were H3K27ac (Diagenode: C15410196) and H3K27me3 (Diagenode: C15410195). For the control input, an IgG antibody (Diagenode code: C15400001-15) was used in each series of ChIP reactions. The input samples consisted of a pooled mixture of all six samples within the respective group.

Sequencing and data analysis

For ATAC-seq and ChIP-seq, paired-end 150bp libraries were sequenced using an Illumina NovaSeq 6000 platform by Novogene Ltd, aiming to generate 40 million reads per sample.

The raw reads were deposited in the European Nucleotide Archive (EBI) and are accessible in the FAANG data coordination centre under accession numbers PRJEB50077 and PRJEB56698 for ATAC-seq and ChIP-seq, respectively. For RNA-seq, we used the differentially expressed data published in Clark et al. (2023), which was from matched samples (EBI accession number: PRJEB50076).

For ATAC-seq and ChIP-seq, the processing of raw reads, mapping of reads, peak calling and quantification was performed using the nextflow pipelines, nf-core/atacseq (v2.0) and nf-core/chipseq (v2.0) (Patel *et al.*, 2020). Raw reads were trimmed using Trim Galore (v0.6.10) and adapters removed. All reads were mapped to the current Atlantic salmon reference genome (GCA_905237065.2) downloaded from the Ensembl genome browser release Ssal_v3.1 (https://www.ensembl.org/Salmo_salar/Info/Index). Mapping was carried out using BWA (v0.7.17) (Li and Durbin, 2009), consensus peak calling for ATAC-seq and ChIP-seq were performed using MACS2 (Zhang *et al.*, 2008). Peaks were annotated using HOMER (v4.9.1) (Heinz *et al*., 2010) and consensus peaks were quantified using featureCounts (Liao et al., 2014). Input controls were included in the peak-calling process to normalize background signal and enhance the specificity of peak identification. The sequence-specific mapping and individually selected genes were visualised using IGV tools (Thorvaldsdottir *et al*., 2013).

The quantified ATAC-Seq and ChIP-Seq peaks were imported into R v4.2.2 (R Core Team, 2022) and differential peak analysis was performed using DESeq2 (Love *et al*., 2014). Significantly different peaks among groups were identified using the Wald test in DESeq2 following False Discovery Rate (FDR) correction using the Benjamini–Hochberg approach, with adjusted *P*-value < 0.05 and up- or down- fold change > 2.

Gene set enrichment analysis

To identify biological processes associated with differentially accessible or modified chromatin regions, we performed region-centric enrichment analysis using the R package

rGREAT (Gu, 2022), which interfaces with the Genomic Regions Enrichment of Annotations Tool. This approach allows functional enrichment analysis directly from genomic coordinates without requiring prior gene assignment, preserving the spatial resolution of the ATAC-seq and ChIP-seq datasets.

Differentially accessible ATAC-seq regions and differentially abundant H3K27ac regions were supplied to rGREAT as query sets in BED format and imported into R as GRanges objects. For each analysis, the background set was defined as the full set of consensuses ATAC-seq or H3K27ac peaks, respectively, to control for assay-specific genomic coverage and avoid biases from using the whole genome as background. Enrichment was tested against Gene Ontology Biological Process (GO:BP) terms using the Atlantic salmon genome annotation (GTF file) and the Ensembl *Salmo salar* dataset (ssalar_gene_ensembl) provided by rGREAT. GO terms with an adjusted *P*-value < 0.05 were considered significantly enriched. In addition, gene expression–centric enrichment analysis was performed using the Database of Annotation, Visualization, and Integrated Discovery (DAVID) (v2023q4) (Huang *et al*., 2009) on the list of differentially expressed genes identified by RNA-seq. Human orthologs of the Atlantic salmon genes were identified following the approach of Clark et al. (2023). In cases where multiple paralogs were expressed for a single gene, the paralog with the highest expression was selected. The background gene set for DAVID was the human gene repertoire. GO terms with fold enrichment > 2 and FDR-adjusted p < 0.05 were considered enriched.

Chromatin state discovery

ChromHMM (v1.24) was used to identify genome-wide chromatin states using the integrated ATAC-seq, H3K27ac and H3K27me3 ChIP-seq datasets. ChromHMM uses a multivariate Hidden Markov Model that considers the spatial and combinatorial arrangements of various chromatin marks to learn and describe these states (Ernst and Kellis, 2012). Firstly, the aligned reads for each sample were converted into a binarized format using the BinarizeBam function using the following command: java -mx4000M -jar ChromHMM.jar BinarizeBam

CHROMSIZES/Ssal_v3.1.txt inputbam samplefile.txt binarize outputdir. We then used the LearnModel function to develop models of chromatin states based on these binary files, automatically generating chromatin state segmentation across the genome. To start model learning and have automatic enrichments computed after the model is learned, the LearnModel command was computed: java -mx4000M -jar ChromHMM.jar LearnModel -p 64 inputdir outputdir 5 Ssal_v3.1. Chromatin states were annotated by ChromHMM using the five-state model based on enrichment of ATAC-seq and H3K27ac signals (active) or H3K27me3 signal (repressive). Promoter regions were defined as the chromatin segments annotated by ChromHMM as promoter-like states and overlapping the annotated transcription start sites (TSSs) from the *Salmo salar* genome annotation. TSS coordinates were derived directly from the reference GTF and correspond to the 5′ end of each transcript.

Transcriptional factor binding site analysis

For the transcription factor binding site (TFBS) prediction and analysis we used GimmeMotifs (Bruse and van Heeringen, 2018) with the JASPAR2022 vertebrate core database (Castro-Mondragon *et al*., 2022), the database comprises curated, non-redundant binding motifs derived from experimental evidence. Motif enrichment was assessed using active regulatory regions from ChromHMM state 5 (active enhancers and promoters) in poly I:C-stimulated and control PBS samples. To reduce false positives, background-matched genomic regions were used, and a *Z*-score threshold of >2 was applied to retain only significantly enriched motifs associated with antiviral responses.

Data access

The raw sequence data has been submitted to the European Nucleotide Archive (ENA) (https://www.ebi.ac.uk/ena/browser/home) under accession numbers PRJEB50076 (RNA-seq), PRJEB50077 (ATAC-seq), and PRJEB56698 (ChIP-seq). Metadata from this study

712 can be found at the AQUA-FAANG Data Portal (https://data.faang.org/projects/AQUA-
713 FAANG).

714 **Competing interest statement**

715 The authors declare no competing interests.

716 **Acknowledgments**

717 This work was funded by the European Union's Horizon 2020 research and innovation
718 program under grant agreement No 817923 (AQUAFAANG) and BBSRC project
719 BB/W008564/1.

720 **Author contributions**

721 **Shahmir Naseer:** Conceptualization, Methodology, Investigation, Data curation, Writing –
722 original draft, Writing – review & editing. **Thomas Clark:** Conceptualization, Methodology,
723 Investigation, Data curation, Writing – original draft, Writing – review & editing. **Daniel J.**
724 **Macqueen:** Conceptualization, Methodology, Investigation, Data curation, Supervision,
725 Funding acquisition, Writing – original draft, Writing – review & editing. **Damir Baranašić**
726 Methodology, Writing – review & editing**. Bertrand Collet**: Conceptualization, Methodology,
727 Investigation, Writing – review & editing. **Pooran Dewari**: Methodology, Investigation, Data
728 curation, Writing – review & editing. **Pierre Boudinot:** Conceptualization, Methodology,
729 Investigation, Data curation, Supervision, Funding acquisition, Writing – original draft, Writing
730 – review & editing. **Samuel A.M. Martin** Conceptualization, Methodology, Investigation, Data
731 curation, Supervision, Funding acquisition, Writing – original draft, Writing – review & editing.

732

733

References

An, L.L., Gong, X.Y., Dan, C., Sun, H.Y., Guo, W.H., Luan, H.Y., Wu, M.Y., Yu, J.C. and Zhang, Y.B., 2025. Family evolution and functional divergence of bony fish-specific Gig1 homologs. Water Biology and Security, p.100382. Available at: https://doi.org/10.1016/j.watbs.2025.100382.

Andresen, A.M., Taylor, R.S., Grimholt, U., Daniels, R.R., Sun, J., Dobie, R., Henderson, N.C., Martin, S.A., Macqueen, D.J. and Fosse, J.H., 2024. Mapping the cellular landscape of Atlantic salmon head kidney by single cell and single nucleus transcriptomics. Fish & shellfish immunology, 146, p.109357. Available at: https://doi.org/10.1016/j.fsi.2024.109357.

Au, W.C. *et al.* (1995) 'Identification of a member of the interferon regulatory factor family that binds to the interferon-stimulated response element and activates expression of interferon-induced genes.', *Proceedings of the National Academy of Sciences*, 92(25), pp. 11657–11661. Available at: https://doi.org/10.1073/pnas.92.25.11657.

Aunsmo, A. *et al.* (2023) 'Real-time monitoring of cause-specific mortality- and losses in industrial salmon farming', *Aquaculture*, 563, p. 738969. Available at: https://doi.org/10.1016/j.aquaculture.2022.738969.

Au-Yeung, N., Mandhana, R. and Horvath, C.M. (2013) 'Transcriptional regulation by STAT1 and STAT2 in the interferon JAK-STAT pathway', *JAK-STAT*, 2(3), p. e23931. Available at: https://doi.org/10.4161/jkst.23931.

Bahrami, S. and Drabløs, F. (2016) 'Gene regulation in the immediate-early response process', Advances in Biological Regulation, 62, pp. 37–49. doi:10.1016/j.jbior.2016.05.001.

Barral, A. and Déjardin, J., 2023. The chromatin signatures of enhancers and their dynamic regulation. Nucleus, 14(1), p.2160551. Available at: https://doi.org/10.1080/19491034.2022.2160551.

Barski, A. *et al.* (2007) 'High-Resolution Profiling of Histone Methylations in the Human Genome', *Cell*, 129(4), pp. 823–837. Available at: https://doi.org/10.1016/j.cell.2007.05.009.

Becker, A.M., Michael, D.G., Satpathy, A.T., Sciammas, R., Singh, H. and Bhattacharya, D., 2012. IRF-8 extinguishes neutrophil production and promotes dendritic cell lineage commitment in both myeloid and lymphoid mouse progenitors. Blood, The Journal of the American Society of Hematology, 119(9), pp.2003-2012. Available at: https://doi.org/10.1182/blood-2011-06-364976.

Bernstein, B.E. *et al.* (2006) 'A Bivalent Chromatin Structure Marks Key Developmental Genes in Embryonic Stem Cells', *Cell*, 125(2), pp. 315–326. Available at: https://doi.org/10.1016/j.cell.2006.02.041.

Biacchesi, S., LeBerre, M., Lamoureux, A., Louise, Y., Lauret, E., Boudinot, P. and Brémont, M., 2009. Mitochondrial antiviral signaling protein plays a major role in induction of the fish innate immune response against RNA and DNA viruses. Journal of virology, 83(16), pp.7815-7827. Available at: https://doi.org/10.1128/jvi.00404-09.

Boison, S. *et al.* (2019) 'QTLs Associated with Resistance to Cardiomyopathy Syndrome in Atlantic Salmon', *Journal of Heredity*. Edited by F. Reed, 110(6), pp. 727–737. Available at: https://doi.org/10.1093/jhered/esz042.

775 Bosselut, R., 2016. Pleiotropic functions of H3K27Me3 demethylases in immune cell
776 differentiation. Trends in immunology, 37(2), pp.102-113. Available at: doi:
777 10.1016/j.it.2015.12.004

778 Briolat, V. *et al.* (2014) 'Contrasted Innate Responses to Two Viruses in Zebrafish: Insights
779 into the Ancestral Repertoire of Vertebrate IFN-Stimulated Genes', *The Journal of*
780 *Immunology*, 192(9), pp. 4328–4341. Available at:
781 https://doi.org/10.4049/jimmunol.1302611.

782 Boudinot P, Salhi S, Blanco M, Benmansour A. Viral haemorrhagic septicaemia virus
783 induces vig-2, a new interferon-responsive gene in rainbow trout. Fish Shellfish Immunol.
784 2001 Jul;11(5):383-97. Available at: doi: 10.1006/fsim.2000.0326. PMID: 11478515.

785 Bruse, N. and Heeringen, S.J. van (2018) *GimmeMotifs: an analysis framework for*
786 *transcription factor motif analysis*. preprint. Bioinformatics. Available at:
787 https://doi.org/10.1101/474403.

788 Buenrostro, J.D. *et al.* (2015) 'ATAC-seq: A method for assaying chromatin accessibility
789 genome-wide', *Current Protocols in Molecular Biology*. Available at:
790 https://doi.org/10.1002/0471142727.mb2129s109.

791 Caprara, G., Prosperini, E., Piccolo, V., Sigismondo, G., Melacarne, A., Cuomo, A., Boothby,
792 M., Rescigno, M., Bonaldi, T. and Natoli, G., 2018. PARP14 controls the nuclear
793 accumulation of a subset of type I IFN–inducible proteins. The Journal of Immunology,
794 200(7), pp.2439-2454. Available at: https://doi.org/10.4049/jimmunol.1701117.

795 Carpenter, S., Ricci, E., Mercier, B. et al. Post-transcriptional regulation of gene expression
796 in innate immunity. Nat Rev Immunol 14, 361–376 (2014). Available at:
797 https://doi.org/10.1038/nri3682

798 Castro, R. *et al.* (2008) 'Characterisation of γ-interferon responsive promoters in fish',
799 *Molecular Immunology*, 45(12), pp. 3454–3462. Available at:
800 https://doi.org/10.1016/j.molimm.2008.03.015.

801 Castro, R. *et al.* (2010) 'Establishment of an IFN-γ specific reporter cell line in fish', *Fish &*
802 *Shellfish Immunology*, 28(2), pp. 312–319. Available at:
803 https://doi.org/10.1016/j.fsi.2009.11.010.

804 Castro-Mondragon, J.A. *et al.* (2022) 'JASPAR 2022: the 9th release of the open-access
805 database of transcription factor binding profiles', *Nucleic Acids Research*, 50(D1), pp. D165–
806 D173. Available at: https://doi.org/10.1093/nar/gkab1113.

807 Chang, C.J., Gu, J. and Robertsen, B. (2017) 'Protective effect and antibody response of
808 DNA vaccine against salmonid alphavirus 3 (SAV3) in Atlantic salmon', *Journal of Fish*
809 *Diseases*, 40(12), pp. 1775–1781. Available at: https://doi.org/10.1111/jfd.12644.

810 Clark, T. *et al.* (2023) 'Conserved and divergent arms of the antiviral response in the
811 duplicated genomes of salmonid fishes', *Genomics*, p. 110663. Available at:
812 https://doi.org/10.1016/j.ygeno.2023.110663.

813 Clark, T.C., Boudinot, P. and Collet, B. (2021) 'Evolution of the IRF family in Salmonids',
814 *Genes*, 12(2), pp. 1–17. Available at: https://doi.org/10.3390/genes12020238.

815 Collet, B. (2004) 'An Mx1 promoter–reporter system to study interferon pathways in rainbow
816 trout', *Developmental & Comparative Immunology*, 28(7–8), pp. 793–801. Available at:
817 https://doi.org/10.1016/j.dci.2003.12.005.

Collet, B. *et al.* (2009) 'Isolation and expression profile of a gene encoding for the Signal Transducer and Activator of Transcription STAT2 in Atlantic salmon (Salmo salar)', *Developmental & Comparative Immunology*, 33(7), pp. 821–829. Available at: https://doi.org/10.1016/j.dci.2009.01.007.

Collet, B. and Secombes, C.J. (2001) 'The rainbow trout (Oncorhynchus mykiss) Mx1 promoter', *European Journal of Biochemistry*, 268(6), pp. 1577–1584. Available at: https://doi.org/10.1046/j.1432-1327.2001.02021.x.

Collins, C., Ganne, G. and Collet, B. (2014) 'Isolation and activity of the promoters for STAT1 and 2 in Atlantic salmon Salmo salar', *Fish & Shellfish Immunology*, 40(2), pp. 644–647. Available at: https://doi.org/10.1016/j.fsi.2014.07.025.

Cooper, L., Xu, H., Polmear, J., Kealy, L., Szeto, C., Pang, E.S., Gupta, M., Kirn, A., Taylor, J.J., Jackson, K.J. and Broomfield, B.J., 2024. Type I interferons induce an epigenetically distinct memory B cell subset in chronic viral infection. Immunity, 57(5), pp.1037-1055. Available at: https://doi.org/10.1016/j.immuni.2024.03.016.

Creyghton, M.P. *et al.* (2010) 'Histone H3K27ac separates active from poised enhancers and predicts developmental state', *Proceedings of the National Academy of Sciences of the United States of America* [Preprint]. Available at: https://doi.org/10.1073/pnas.1016071107.

Dehler, C.E. *et al.* (2023) 'Phylogeny and expression of tetraspanin CD9 paralogues in rainbow trout (Oncorhynchus mykiss)', *Developmental & Comparative Immunology*, 146, p. 104735. Available at: https://doi.org/10.1016/j.dci.2023.104735.

Elias, S. *et al.* (2018) 'Blimp-1/PRDM1 is a critical regulator of Type III Interferon responses in mammary epithelial cells', *Scientific Reports*, 8(1), p. 237. Available at: https://doi.org/10.1038/s41598-017-18652-9.

Ernst, J. and Kellis, M. (2012) 'ChromHMM: automating chromatin-state discovery and characterization', *Nature Methods*, 9(3), pp. 215–216. Available at: https://doi.org/10.1038/nmeth.1906.

Ernst, J. and Kellis, M. (2017) 'Chromatin-state discovery and genome annotation with ChromHMM', *Nature Protocols*, 12(12), pp. 2478–2492. Available at: https://doi.org/10.1038/nprot.2017.124.

Gan, Z. *et al.* (2020) 'Fish type I and type II interferons: composition, receptor usage, production and function', *Reviews in Aquaculture*, 12(2), pp. 773–804. Available at: https://doi.org/10.1111/raq.12349.

Gillard, G.B. *et al.* (2021) 'Comparative regulomics supports pervasive selection on gene dosage following whole genome duplication', *Genome Biology*, 22(1), p. 103. Available at: https://doi.org/10.1186/s13059-021-02323-0.

Gu, Z. and Hübschmann, D., 2023. rGREAT: an R/bioconductor package for functional enrichment on genomic regions. Bioinformatics, 39(1), p.btac745. Available at: https://doi.org/10.1093/bioinformatics/btac745.

Haller, O., Stertz, S. and Kochs, G., 2007. The Mx GTPase family of interferon-induced antiviral proteins. *Microbes and infection*, *9*(14-15), pp.1636-1643. Available at: https://doi.org/10.1016/j.micinf.2007.09.010.

Hambleton, S., Salem, S., Bustamante, J., Bigley, V., Boisson-Dupuis, S., Azevedo, J., Fortin, A., Haniffa, M., Ceron-Gutierrez, L., Bacon, C.M., Menon, G., Trouillet, C., McDonald,

D., Carey, P., Ginhoux, F., Alsina, L., Zumwalt, T.J., Kong, X.F., Kumararatne, D., Butler, K., Hubeau, M., Feinberg, J., Al-Muhsen, S., Cant, A., Abel, L., Chaussabel, D., Doffinger, R., Talesnik, E., Grumach, A., Duarte, A., Abarca, K., Moraes-Vasconcelos, D., Burk, D., Berghuis, A., Geissmann, F., Collin, M., Casanova, J.L. and Gros, P., 2011. IRF8 mutations and human dendritic-cell immunodeficiency. The New England Journal of Medicine, 365(2), pp.127-138.

Harshil Patel *et al.* (2020) 'nf-core/chipseq: nf-core/chipseq v1.2.1 - Platinum Mole'. Zenodo. Available at: https://doi.org/10.5281/ZENODO.3966161.

Harshil Patel *et al.* (2022) 'nf-core/atacseq: nf-core/atacseq v2.0 - Iron Iguana'. Zenodo. Available at: https://doi.org/10.5281/ZENODO.2634132.

Harvey, T.N., Gillard, G.B., Røsæg, L.L., Grammes, F., Monsen, Ø., Vik, J.O., Hvidsten, T.R. and Sandve, S.R., 2024. The genome regulatory landscape of Atlantic salmon liver through smoltification. Plos one, 19(4), p.e0302388. Available at: https://doi.org/10.1371/journal.pone.0302388.

Heinz, S., Benner, C., Spann, N., Bertolino, E., Lin, Y.C., Laslo, P., Cheng, J.X., Murre, C., Singh, H. and Glass, C.K., 2010. Simple combinations of lineage-determining transcription factors prime cis-regulatory elements required for macrophage and B cell identities. Molecular cell, 38(4), pp.576-589. Available at: https://doi.org/10.1016/j.molcel.2010.05.004.

Holland, J.W. *et al.* (2008) 'Molecular characterization of IRF3 and IRF7 in rainbow trout, Oncorhynchus mykiss: Functional analysis and transcriptional modulation', *Molecular Immunology*, 46(2), pp. 269–285. Available at: https://doi.org/10.1016/j.molimm.2008.08.265.

Houston, R.D. *et al.* (2010) 'The susceptibility of Atlantic salmon fry to freshwater infectious pancreatic necrosis is largely explained by a major QTL', *Heredity*, 105(3), pp. 318–327. Available at: https://doi.org/10.1038/hdy.2009.171.

Houston, R.D. *et al.* (2020) 'Harnessing genomics to fast-track genetic improvement in aquaculture', *Nature Reviews Genetics*, 21(7), pp. 389–409. Available at: https://doi.org/10.1038/s41576-020-0227-y.

Huang, D.W., Sherman, B.T. and Lempicki, R.A. (2009) 'Systematic and integrative analysis of large gene lists using DAVID bioinformatics resources', *Nature Protocols*, 4(1), pp. 44–57. Available at: https://doi.org/10.1038/nprot.2008.211.

Huntzinger, E., Izaurralde, E. Gene silencing by microRNAs: contributions of translational repression and mRNA decay. Nat Rev Genet 12, 99–110 (2011). https://doi.org/10.1038/nrg2936.

Islam, M.M. and Zhang, C.-L. (2015) 'TLX: A master regulator for neural stem cell maintenance and neurogenesis', *Biochimica et Biophysica Acta (BBA) - Gene Regulatory Mechanisms*, 1849(2), pp. 210–216. Available at: https://doi.org/10.1016/j.bbagrm.2014.06.001.

Ivashkiv, L.B. and Donlin, L.T. (2014) 'Regulation of type I interferon responses', *Nature Reviews Immunology*, 14(1), pp. 36–49. Available at: https://doi.org/10.1038/nri3581.

Jefferies, C.A. (2019) 'Regulating IRFs in IFN Driven Disease', *Frontiers in Immunology*, 10, p. 325. Available at: https://doi.org/10.3389/fimmu.2019.00325.

903 Jose Priya, T.A. and Kappalli, S. (2022) 'Modern biotechnological strategies for vaccine
904 development in aquaculture – Prospects and challenges', *Vaccine*, 40(41), pp. 5873–5881.
905 Available at: https://doi.org/10.1016/j.vaccine.2022.08.075.

906 Junttila, I.S., 2018. 'Tuning the cytokine responses: an update on interleukin (IL)-4 and IL-13
907 receptor complexes'. Frontiers in immunology, 9, p.888. Available at:
908 https://doi.org/10.3389/fimmu.2018.00888

909 Kan, R.L., Chen, J. and Sallam, T. (2022) 'Crosstalk between epitranscriptomic and
910 epigenetic mechanisms in gene regulation', *Trends in Genetics*, 38(2), pp. 182–193.
911 Available at: https://doi.org/10.1016/j.tig.2021.06.014.

912 Kanehisa, M. *et al.* (2010) 'KEGG for representation and analysis of molecular networks
913 involving diseases and drugs', *Nucleic Acids Research*, 38(suppl_1), pp. D355–D360.
914 Available at: https://doi.org/10.1093/nar/gkp896.

915 Kell, A.M. and Gale, M. (2015) 'RIG-I in RNA virus recognition', *Virology*, 479–480, pp. 110–
916 121. Available at: https://doi.org/10.1016/j.virol.2015.02.017.

917 Koepke, L., Gack, M.U. and Sparrer, K.M., 2021. The antiviral activities of TRIM proteins.
918 Current opinion in microbiology, 59, pp.50-57. Available at:
919 https://doi.org/10.1016/j.mib.2020.07.005.

920 Laidlaw, B.J., Cyster, J.G. Transcriptional regulation of memory B cell differentiation. Nat
921 Rev Immunol 21, 209–220 (2021). https://doi.org/10.1038/s41577-020-00446-2. Laricchia-
922 Robbio, L., Tamura, T., Karpova, T., Sprague, B.L., McNally, J.G. and Ozato, K., 2005.
923 Partner-regulated interaction of IFN regulatory factor 8 with chromatin visualized in live
924 macrophages. Proceedings of the National Academy of Sciences, 102(40), pp.14368-14373.

925 Langevin C, Boudinot P, Collet B. IFN Signaling in Inflammation and Viral Infections: New
926 Insights from Fish Models. Viruses. 2019 Mar 26;11(3):302. doi: 10.3390/v11030302.

927 Levraud, J.-P. *et al.* (2019) 'IFN-Stimulated Genes in Zebrafish and Humans Define an
928 Ancient Arsenal of Antiviral Immunity', *The Journal of Immunology*, 203(12), pp. 3361–3373.
929 Available at: https://doi.org/10.4049/jimmunol.1900804.

930 Li, B. and Dewey, C.N. (2011) 'RSEM: accurate transcript quantification from RNA-seq data
931 with or without a reference genome', *BMC Bioinformatics*, 12(1), p. 323. Available at:
932 https://doi.org/10.1186/1471-2105-12-323.

933 Li, D. and Wu, M. (2021) 'Pattern recognition receptors in health and diseases', *Signal
934 Transduction and Targeted Therapy*, 6(1), p. 291. Available at:
935 https://doi.org/10.1038/s41392-021-00687-0.

936 Li, H. and Durbin, R. (2009) 'Fast and accurate short read alignment with Burrows–Wheeler
937 transform', *Bioinformatics*, 25(14), pp. 1754–1760. Available at:
938 https://doi.org/10.1093/bioinformatics/btp324.

939 Li, J., Rodriguez, J.P., Niu, F., Pu, M., Wang, J., Hung, L.W., Shao, Q., Zhu, Y., Ding, W.,
940 Liu, Y. and Da, Y., 2016. Structural basis for DNA recognition by STAT6. Proceedings of the
941 National Academy of Sciences, 113(46), pp.13015-13020. Available at:
942 https://doi.org/10.1073/pnas.1611228113.

943 Liang, Y. *et al.* (2022) 'Negative regulation of interferon regulatory factor 6 (IRF6) in
944 interferon and NF-κB signalling pathways of common carp (Cyprinus carpio L.)', *BMC*

Veterinary Research, 18(1), p. 433. Available at: https://doi.org/10.1186/s12917-022-03538-4.

Liao, Y., Smyth, G.K. and Shi, W. (2014) 'featureCounts: an efficient general purpose program for assigning sequence reads to genomic features', *Bioinformatics*, 30(7), pp. 923–930. Available at: https://doi.org/10.1093/bioinformatics/btt656.

Lien, S. *et al.* (2016) 'The Atlantic salmon genome provides insights into rediploidization', *Nature* [Preprint]. Available at: https://doi.org/10.1038/nature17164.

Lin Y, Wong K, Calame K. Repression of c-myc transcription by Blimp-1, an inducer of terminal B cell differentiation. Science. 1997 Apr 25;276(5312):596-9. doi: 10.1126/science.276.5312.596.

Liu, T. *et al.* (2017) 'NF-κB signaling in inflammation', *Signal Transduction and Targeted Therapy*, 2(1), p. 17023. Available at: https://doi.org/10.1038/sigtrans.2017.23.

Liu, Y.-J. (2005) 'IPC: Professional Type 1 Interferon-Producing Cells and Plasmacytoid Dendritic Cell Precursors', *Annual Review of Immunology*, 23(1), pp. 275–306. Available at: https://doi.org/10.1146/annurev.immunol.23.021704.115633.

Love, M.I., Huber, W. and Anders, S. (2014) 'Moderated estimation of fold change and dispersion for RNA-seq data with DESeq2', *Genome Biology*, 15(12), p. 550. Available at: https://doi.org/10.1186/s13059-014-0550-8.

Lukacs, M.F., Harstad, H., Bakke, H.G., Beetz-Sargent, M., McKinnel, L., Lubieniecki, K.P., Koop, B.F. and Grimholt, U., 2010. Comprehensive analysis of MHC class I genes from the U-, S-, and Z-lineages in Atlantic salmon. BMC genomics, 11(1), p.154. Available at: https://doi.org/10.1186/1471-2164-11-154.

Mancino A, Termanini A, Barozzi I, Ghisletti S, Ostuni R, Prosperini E, Ozato K, Natoli G. A dual cis-regulatory code links IRF8 to constitutive and inducible gene expression in macrophages. Genes Dev. 2015 Feb 15;29(4):394-408. doi: 10.1101/gad.257592.114.

Martin, S.A.M. *et al.* (2007) 'Interferon type I and type II responses in an Atlantic salmon (Salmo salar) SHK-1 cell line by the salmon TRAITS/SGP microarray', *Physiological Genomics*, 32(1), pp. 33–44. Available at: https://doi.org/10.1152/physiolgenomics.00064.2007.

Maruyama, K. *et al.* (2012) 'The Transcription Factor Jdp2 Controls Bone Homeostasis and Antibacterial Immunity by Regulating Osteoclast and Neutrophil Differentiation', *Immunity*, 37(6), pp. 1024–1036. Available at: https://doi.org/10.1016/j.immuni.2012.08.022.

Matsumoto, M. *et al.* (2003) 'Subcellular Localization of Toll-Like Receptor 3 in Human Dendritic Cells', *The Journal of Immunology*, 171(6), pp. 3154–3162. Available at: https://doi.org/10.4049/jimmunol.171.6.3154.

McNab, F. *et al.* (2015) 'Type I interferons in infectious disease', *Nature Reviews Immunology*, 15(2), pp. 87–103. Available at: https://doi.org/10.1038/nri3787.

Mondal, H. and Thomas, J. (2022) 'A review on the recent advances and application of vaccines against fish pathogens in aquaculture', *Aquaculture International* [Preprint]. Available at: https://doi.org/10.1007/s10499-022-00884-w.

Moorman, H.R., Reategui, Y., Poschel, D.B. and Liu, K., 2022. IRF8: mechanism of action and health implications. Cells, 11(17), p.2630. Available at: https://doi.org/10.3390/cells11172630.

Mostafavi, S. *et al.* (2016) 'Parsing the Interferon Transcriptional Network and Its Disease Associations', *Cell*, 164(3), pp. 564–578. Available at: https://doi.org/10.1016/j.cell.2015.12.032.

Murphy A.E. *et al* (2024) 'Predicting gene expression from histone marks using chromatin deep learning models depends on histone mark function, regulatory distance and cellular states', Nucleic Acids Research, gkae1212. Available at: https://doi.org/10.1093/nar/gkae1212.

Naylor, R.L. *et al.* (2021) 'A 20-year retrospective review of global aquaculture', *Nature* |, 591, p. 551. Available at: https://doi.org/10.1038/s41586-021-03308-6.

Perdiguero, P. *et al.* (2020) 'Insights Into the Evolution of the prdm1/Blimp1 Gene Family in Teleost Fish', *Frontiers in Immunology*, 11, p. 596975. Available at: https://doi.org/10.3389/fimmu.2020.596975.

Platanias, L.C. (2005) 'Mechanisms of type-I- and type-II-interferon-mediated signalling', *Nature Reviews Immunology*, 5(5), pp. 375–386. Available at: https://doi.org/10.1038/nri1604.

Platanitis, E. *et al.* (2019) 'A molecular switch from STAT2-IRF9 to ISGF3 underlies interferon-induced gene transcription', *Nature Communications*, 10(1), p. 2921. Available at: https://doi.org/10.1038/s41467-019-10970-y.

R Core Team (2022) R: A language and environment for statistical computing. Vienna: R Foundation for Statistical Computing. Available at: https://www.R-project.org/.

Rehwinkel, J. and Gack, M.U. (2020) 'RIG-I-like receptors: their regulation and roles in RNA sensing', *Nature Reviews Immunology*, 20(9), pp. 537–551. Available at: https://doi.org/10.1038/s41577-020-0288-3.

Robertson, F.M. *et al.* (2017) 'Lineage-specific rediploidization is a mechanism to explain time-lags between genome duplication and evolutionary diversification', *Genome Biology*, 18(1), p. 111. Available at: https://doi.org/10.1186/s13059-017-1241-z.

Schoggins, J.W. *et al.* (2011) 'A diverse range of gene products are effectors of the type I interferon antiviral response', *Nature*, 472(7344), pp. 481–485. Available at: https://doi.org/10.1038/nature09907.

Schoggins, J.W. (2019) 'Interferon-Stimulated Genes: What Do They All Do?', *Annual Review of Virology*, 6(1), pp. 567–584. Available at: https://doi.org/10.1146/annurev-virology-092818-015756.

Skjesol, A. *et al.* (2010) 'Structural and functional studies of STAT1 from Atlantic salmon (Salmo salar)', *BMC Immunology*, 11(1), p. 17. Available at: https://doi.org/10.1186/1471-2172-11-17.

Takeuchi, O. and Akira, S. (2008) 'MDA5/RIG-I and virus recognition', *Current Opinion in Immunology*, 20(1), pp. 17–22. Available at: https://doi.org/10.1016/j.coi.2008.01.002.

Tamura T, Kurotaki D, Koizumi S. Regulation of myelopoiesis by the transcription factor IRF8. Int J Hematol. 2015 Apr;101(4):342-51. doi: 10.1007/s12185-015-1761-9.

Tan, Q., Wang, J., Hao, Y., Yang, S., Cao, B., Pan, W. and Cao, M., 2025. Elf1 Deficiency Impairs Macrophage Development in Zebrafish Model Organism. International Journal of Molecular Sciences, 26(6), p.2537. Available at: https://doi.org/10.3390/ijms26062537.

Taylor, R.S., Ruiz Daniels, R., Dobie, R., Naseer, S., Clark, T.C., Henderson, N.C., Boudinot, P., Martin, S.A. and Macqueen, D.J., 2022. Single cell transcriptomics of Atlantic salmon (*Salmo salar* L.) liver reveals cellular heterogeneity and immunological responses to challenge by Aeromonas salmonicida. Frontiers in immunology, 13, p.984799. Available at: https://doi.org/10.3389/fimmu.2022.984799.

Tena, J.J. and Santos-Pereira, J.M., 2021. Topologically associating domains and regulatory landscapes in development, evolution and disease. Frontiers in cell and developmental biology, 9, p.702787. Available at: https://doi.org/10.3389/fcell.2021.702787.

Thompson, M.R., Kaminski, J.J., Kurt-Jones, E.A. and Fitzgerald, K.A., 2011. Pattern recognition receptors and the innate immune response to viral infection. Viruses, 3(6), p.920. doi: 10.3390/v3060920.

Thorvaldsdottir, H., Robinson, J.T. and Mesirov, J.P. (2013) 'Integrative Genomics Viewer (IGV): high-performance genomics data visualization and exploration', *Briefings in Bioinformatics*, 14(2), pp. 178–192. Available at: https://doi.org/10.1093/bib/bbs017.

Tsai, D.-Y. *et al.* (2019) 'Regulatory mechanisms of B cell responses and the implication in B cell-related diseases', *Journal of Biomedical Science*, 26(1), p. 64. Available at: https://doi.org/10.1186/s12929-019-0558-1.

Uzé, G. *et al.* (2007) 'The Receptor of the Type I Interferon Family', in P.M. Pitha (ed.) *Interferon: The 50th Anniversary*. Berlin, Heidelberg: Springer Berlin Heidelberg (Current Topics in Microbiology and Immunology), pp. 71–95. Available at: https://doi.org/10.1007/978-3-540-71329-6_5.

van Der Aa, L.M., Levraud, J.P., Yahmi, M., Lauret, E., Briolat, V., Herbomel, P., Benmansour, A. and Boudinot, P., 2009. A large new subset of TRIM genes highly diversified by duplication and positive selection in teleost fish. BMC biology, 7(1), p.7. Available at: https://doi.org/10.1186/1741-7007-7-7.

Wang, B. *et al.* (2014) 'Fish viperin exerts a conserved antiviral function through RLR-triggered IFN signaling pathway', *Developmental & Comparative Immunology*, 47(1), pp. 140–149. Available at: https://doi.org/10.1016/j.dci.2014.07.006.

Wang, W. *et al.* (2017) 'Transcriptional Regulation of Antiviral Interferon-Stimulated Genes', *Trends in Microbiology*, 25(7), pp. 573–584. Available at: https://doi.org/10.1016/j.tim.2017.01.001.

Wang, Z. *et al.* (2008) 'Combinatorial patterns of histone acetylations and methylations in the human genome', *Nature Genetics*, 40(7), pp. 897–903. Available at: https://doi.org/10.1038/ng.154.

Yanong, R.P.E. and Erlacher-Reid, C. (2012) 'Biosecurity in Aquaculture, Part 1: An Overview', (4707), p. 522.

Zhang, Y. *et al.* (2008) 'Model-based Analysis of ChIP-Seq (MACS)', *Genome Biology*, 9(9), p. R137. Available at: https://doi.org/10.1186/gb-2008-9-9-r137.

Zou, J. and Secombes, C.J. (2011) 'Teleost fish interferons and their role in immunity', *Developmental & Comparative Immunology*, 35(12), pp. 1376–1387. Available at: https://doi.org/10.1016/j.dci.2011.07.001.

Table 1. 54 conserved ISGs common between ATAC-seq, ChIP-seq (H3K27ac) and RNA-seq. Considered ISG data was obtained from Clark et al, (2023).

Ensembl id	FC ATAC	FC H3K27ac	FC RNA	HGNC	Description
ENSSSAG00000068365	4.16	1.62	5.64	IFIT5	interferon induced protein with tetratricopeptide repeats 5
ENSSSAG00000064740	3.35	2.16	4.49	UBB	ubiquitin B
ENSSSAG00000077530	2.79	2.35	4.58	MX1	MX dynamin like GTPase 1
ENSSSAG00000041408	2.75	3.29	4.12	RNF213	ring finger protein 213
ENSSSAG00000043101	2.72	1.62	5.39	BATF	Basic Leucine Zipper ATF-Like Transcription Factor
ENSSSAG00000108395	2.58	3.09	4.54	SAMD9	sterile alpha motif domain containing 9
ENSSSAG00000118579	2.55	3.88	4.88	SOCS1	suppressor of cytokine signaling 1
ENSSSAG00000104513	2.44	3.46	4.79	SOCS1	suppressor of cytokine signaling 1
ENSSSAG00000043265	2.40	1.84	4.91	HERC3	HECT and RLD domain containing E3 ubiquitin protein ligase 3
ENSSSAG00000007886	2.39	2.24	5.22	CMPK2	cytidine/uridine monophosphate kinase 2
ENSSSAG00000073332	2.21	1.55	3.01	HELZ2	helicase with zinc finger 2
ENSSSAG00000121778	2.04	1.12	5.49	UBB	ubiquitin B
ENSSSAG00000058932	2.02	1.95	3.22	PARP14	poly(ADP-ribose) polymerase family member 14
ENSSSAG00000078539	2.02	1.55	1.66	RNF213	ring finger protein 213
ENSSSAG00000056446	1.98	1.86	3.79	NLRC5	NLR family CARD domain containing 5
ENSSSAG00000077480	1.96	1.71	4.64	NAMPT	nicotinamide phosphoribosyltransferase
ENSSSAG00000043036	1.94	1.54	4.24	ZNFX1	zinc finger NFX1-type containing 1
ENSSSAG00000075304	1.92	1.69	2.98	EIF2AK2	eukaryotic translation initiation factor 2 alpha kinase 2
ENSSSAG00000005181	1.85	1.48	3.31	SAMD9L	sterile alpha motif domain containing 9 like
ENSSSAG00000054938	1.82	1.85	2.51	PARP12	poly [ADP-ribose] polymerase 12-like
ENSSSAG00000071823	1.77	2.65	2.48	XCL2	X-C motif chemokine ligand 2
ENSSSAG00000110347	1.77	1.32	5.65	TREX	three prime repair exonuclease
ENSSSAG00000079036	1.74	2.05	4.92	IFIT5	interferon induced protein with tetratricopeptide repeats 5
ENSSSAG00000072910	1.70	2.31	3.17	IFI44L	interferon induced protein 44 like
ENSSSAG00000068298	1.66	1.59	1.48	NLRC5	NLR family CARD domain containing 5
ENSSSAG00000059637	1.65	1.19	1.75	TSPAN33	tetraspanin 33
ENSSSAG00000004551	1.63	1.74	3.08	XAF1	XIAP associated factor 1
ENSSSAG00000003156	1.62	1.66	5.13	DHX58	DExH-box helicase 58
ENSSSAG00000075036	1.62	2.35	3.40	LGALS3BP	galectin 3 binding protein
ENSSSAG00000081672	1.61	1.21	3.48	PARP9	poly(ADP-ribose) polymerase family member 9
ENSSSAG00000049790	1.55	1.82	3.25	LGALS9C	galectin 9C
ENSSSAG00000046065	1.53	1.59	3.50	USP20	ubiquitin specific peptidase 20
ENSSSAG00000051388	1.52	1.69	4.17	NCOA7	nuclear receptor coactivator 7
ENSSSAG00000005381	1.51	2.31	3.94	PARP12	poly(ADP-ribose) polymerase family member 12
ENSSSAG00000078885	1.48	1.48	2.73	IFIH1	interferon induced with helicase C domain 1
ENSSSAG00000119673	1.47	1.64	2.54	DDX58	DExD/H-box helicase 58
ENSSSAG00000072880	1.46	1.82	2.93	TRAFD1	TRAF-type zinc finger domain containing 1
ENSSSAG00000054674	1.46	1.43	1.88	RNF213	ring finger protein 213
ENSSSAG00000045256	1.45	1.18	2.69	IFI44	interferon-induced protein 44-like
ENSSSAG00000045959	1.45	1.69	1.94	PARP12	poly(ADP-ribose) polymerase family member 12
ENSSSAG00000048046	1.36	1.39	6.43	RSAD2	radical S-adenosyl methionine domain containing 2
ENSSSAG00000020083	1.34	1.84	2.96	PARP12	poly [ADP-ribose] polymerase 12-like
ENSSSAG00000002526	1.28	1.36	2.92	USP20	ubiquitin specific peptidase 20
ENSSSAG00000077407	1.26	1.25	1.53	TAPBP	TAP binding protein
ENSSSAG00000042163	1.22	1.77	2.42	PARP9	poly(ADP-ribose) polymerase family member 9
ENSSSAG00000037936	1.15	2.03	1.49	LGALS3BP	galectin 3 binding protein
ENSSSAG00000119808	1.14	1.68	2.13	OGFR	opioid growth factor receptor
ENSSSAG00000006364	1.12	1.65	1.76	ADAR	adenosine deaminase RNA specific
ENSSSAG00000001032	1.11	1.50	1.94	RNF114	ring finger protein 114
ENSSSAG00000076373	1.08	1.75	3.37	IRF7	interferon regulatory factor 7
ENSSSAG00000074138	1.06	1.17	2.29	CGAS	cyclic GMP-AMP synthase
ENSSSAG00000058809	1.04	1.59	2.38	PARP15	poly(ADP-ribose) polymerase family member 15
ENSSSAG00000070425	1.03	1.31	1.31	MOV10	Mov10 RISC complex RNA helicase
ENSSSAG00000047562	1.01	1.78	1.58	RNF213	ring finger protein 213

Table 2. Genes with eniched IRF8 (ISRE) motifs identified in a subset of 197 genes that are common among ATAC-seq, H3K27ac ChIP-seq, and RNA-seq datasets. FC RNA indicate the fold change in response to Ploy I:C at mRNA level.

Ensembl_id	HGNC	Description	FC RNA	FDR
ENSSSAG00000099839	ENSSSAG00000099839		3.26	0.000
ENSSSAG00000010621	EDIL3	EGF like repeats and discoidin domains 3	3.33	0.000
ENSSSAG00000044071	CARS1	cysteinyl-tRNA synthetase 1	2.71	0.000
ENSSSAG00000078539	RNF213	ring finger protein 213	3.16	0.000
ENSSSAG00000058809	PARP15	poly(ADP-ribose) polymerase family member 15	5.20	0.000
ENSSSAG00000058932	PARP14	poly(ADP-ribose) polymerase family member 14	9.32	0.000
ENSSSAG00000004437	TDRD3	Tudor Domain Containing 3	12.70	0.000
ENSSSAG00000115088	ENSSSAG00000115088		4.54	0.000
ENSSSAG00000098558	MX1	MX dynamin like GTPase 1	10.61	0.000
ENSSSAG00000074112	ENSSSAG00000074112		4.95	0.000
ENSSSAG00000072910	*IFI44L*	*interferon induced protein 44 like*	*9.01*	*0.000*
ENSSSAG00000112886	RTP4	receptor transporter protein 4	35.48	0.000
ENSSSAG00000085797	RTP3	receptor transporter protein 3	52.11	0.000
ENSSSAG00000045959	PARP12	poly(ADP-ribose) polymerase family member 12	3.82	0.000
ENSSSAG00000089774	ARI6	Putative E3 ubiquitin-protein ligase SINA-like 6	13.42	0.000
ENSSSAG00000061910	TRIM21	tripartite motif containing 21	12.17	0.000
ENSSSAG00000098931	CPRAS1	circularly permutated Ras protein 1-like	5.49	0.000
ENSSSAG00000032869	CALCOCO2	calcium binding and coiled-coil domain 2	2.23	0.000
ENSSSAG00000064740	UBB	ubiquitin B	22.54	0.000
ENSSSAG00000121778	UBB	ubiquitin B	44.79	0.000
ENSSSAG00000078885	IFIH1	interferon induced with helicase C domain 1	6.64	0.000
ENSSSAG00000074688	GIG2P	grass carp reovirus (GCRV)-induced gene 2p	7.09	0.000
ENSSSAG00000042324	TLR7	toll like receptor 7	4.90	0.000
ENSSSAG00000112790	ENSSSAG00000112790		2.39	0.000
ENSSSAG00000001032	RNF114	ring finger protein 114	3.82	0.000
ENSSSAG00000119632	ENSSSAG00000119632		5.56	0.000
ENSSSAG00000008629	HERC3	HECT and RLD domain containing E3 ubiquitin protein ligase 3	3.89	0.000
ENSSSAG00000040462	MEFV	MEFV innate immuity regulator, pyrin	5.21	0.000
ENSSSAG00000120148	URGCP	upregulator of cell proliferation	2.88	0.027
ENSSSAG00000053722	FMR1	FMRP translational regulator 1	2.73	0.000
ENSSSAG00000067713	ZC3H7B	zinc finger CCCH-type containing 7B	2.29	0.000
ENSSSAG00000003892	ENSSSAG00000003892		11.81	0.001
ENSSSAG00000005950	FRK	fyn related Src family tyrosine kinase	5.99	0.000
ENSSSAG00000009694	TRIM35	tripartite motif containing 35	18.23	0.000
ENSSSAG00000043265	HERC3	HECT and RLD domain containing E3 ubiquitin protein ligase 3	30.05	0.000
ENSSSAG00000043072	HERC3	HECT and RLD domain containing E3 ubiquitin protein ligase 3	22.19	0.000
ENSSSAG00000063287	MAVS	mitochondrial antiviral-signaling protein-like	8.54	0.000

Figure Legends:

Figure 1. Genomic distribution of ATAC-seq and H3K27ac ChIP-seq peaks relative to gene features and transcription start sites (TSS). Barplots showing the number of consensus peaks associated with genes or unassociated to genes in ATAC-seq (A) and H3K27ac (B) datasets. Distribution of peak–gene associations binned by signed distance to the nearest TSS in ATAC-seq (C) and H3K27ac (D) datasets. Most peaks are located within 50 kb of a TSS, supporting their annotation as promoters or enhancers.

Figure 2. Integrative analysis of chromatin accessibility, histone modifications, and gene expression following poly I:C stimulation in Atlantic salmon. (A) Genome browser tracks showing ATAC-seq, RNA-seq, and gene annotation at the elf1a locus in PBS (control) and poly I:C–stimulated samples. The housekeeping gene elf1a is shown as a representative locus to illustrate the data quality and consistency across assays. (B) Genome browser tracks at the same locus showing H3K27ac ChIP-seq signal, indicating histone modification in both control and poly I:C stimulated samples. (C) Gene Ontology (GO) biological process enrichment of genes associated with upregulated ATAC-seq peaks. Dot size reflects the number of observed regions; colour scale indicates adjusted *P*-values. (D) GO biological process enrichment of genes associated with upregulated H3K27ac peaks, displayed as in (C). For GO analysis following filtrations were carried out: fold enrichment > 5, observed hits ≥ 10 and p adjusted < 0.05. (E) Volcano plot of differentially accessible ATAC-seq regions between PBS and poly I:C. Red points indicate significantly upregulated regions, green points indicate downregulated regions, black points are not significant. (F) Volcano plot of differentially enriched H3K27ac-marked regions. (G) Volcano plot of differentially enriched H3K27me3-marked regions.

Figure 3. Comparative analysis of the ATAC, ChIP, and RNA-seq data following poly I:C stimulated Atlantic salmon. (A) Venn diagram illustrating the overlap of upregulated genes among the different assays. (B) Gene Ontology analysis of the upregulated genes shared between ATAC, RNA-seq, and ChIP H3K27ac, providing insights into the biological processes associated with these genes and their involvement in the antiviral response. (D) Genes with significant ATAC and H3K27ac presence at regulatory regions but were not significantly expressed at transcript level. (E) Genes which were upregulated at transcript level however their regulatory regions were not significantly activated. (F) Genes which were significantly expressed and had significant H3K27ac peaks. GO analysis was performed using DAVID, with stringent filtering criteria of FDR < 0.05 and fold enrichment > 2.

Figure 4. TFBS analysis of key set of antiviral genes. (A) TFBS identified in a subset of 197 genes that are common among ATAC-seq, H3K27ac ChIP-seq, and RNA-seq datasets. Distribution of TFBS showing that over 20% of the genes contain IRF8 binding sites; the accompanying table 2 lists the gene IDs associated with these IRF8 binding sites. (B) Sequence logo representing the binding motif of IRF8, highlighting the conserved nucleotide positions crucial for IRF8 binding specificity. Transcription factor binding sites were identified using GimmeMotifs from the enriched regions in ATAC-seq and H3K27ac, corresponding to active enhancers and promoters; the JASPER database was used as background.

Figure 5. Transcription factor binding analysis. A, B, and C present the results of ChromHMM chromatin state discovery using ATAC-seq and two ChIP marks (H3K27ac and H3K27me3). (A) The five states predicted by the model are shown and annotated based on existing literature. (B) The genomic location of the segments in each state is depicted for the PBS control samples. (C) The genomic location of the segments in each state is depicted for the poly I:C stimulated samples. (D) Transcription factor binding sites were identified using GimmeMotifs from the enriched regions in state 5, corresponding to active enhancers and

promoters; the JASPER database was used as background. These transcription factors have binding sites enriched in ATAC and H3K27ac, however, GimmeMotif also predicted binding sites of transcription factors enriched from our dataset. For the list of predicted transcription factors, refer to supplementary table 7.

Figure 6. Anti-viral IFN response processes. (A) A schematic view illustrating the type I IFN signalling pathway, encompassing both primary and secondary responses. (B) A table displaying the genes involved in the RIG-I and JAK-STAT pathways, along with their fold change values from the differential gene expression analysis. The colour coding indicates upregulation (red), downregulation (green), and no response (grey). (C) and (D) IGV visualisations of the RIG-I and JAK-STAT pathway genes derived from the ATAC-seq, ChIP-seq, and RNA-seq datasets. The visualisations also include the enriched ISRE motifs associated with each gene. The direction of the gene transcription is indicated by the black arrow below the gene structure.

Figure 7. Visualisation of key anti-viral response genes. (A) Shows the IGV visualisations of ATAC-seq, ChIP-seq, and RNA-seq data for the genes MX2, RSAD2, TAPBP, ISG15, and CD9. The visualisations illustrate the chromatin accessibility, histone modification profiles, and gene expression patterns associated with each gene. Enriched ISRE motifs specific to each gene are identified, indicating their regulatory importance in driving the anti-viral response. Arrows next to the transcripts indicate the direction of the sequence. (B) Presents a table summarising the gene expression data for MX2, RSAD2, TAPBP, ISG15, and CD9. Red indicates upregulation, green indicates downregulation, and grey indicates no response. The table provides a concise overview of the transcriptional changes exhibited by these key anti-viral response genes following stimulation with poly I:C.

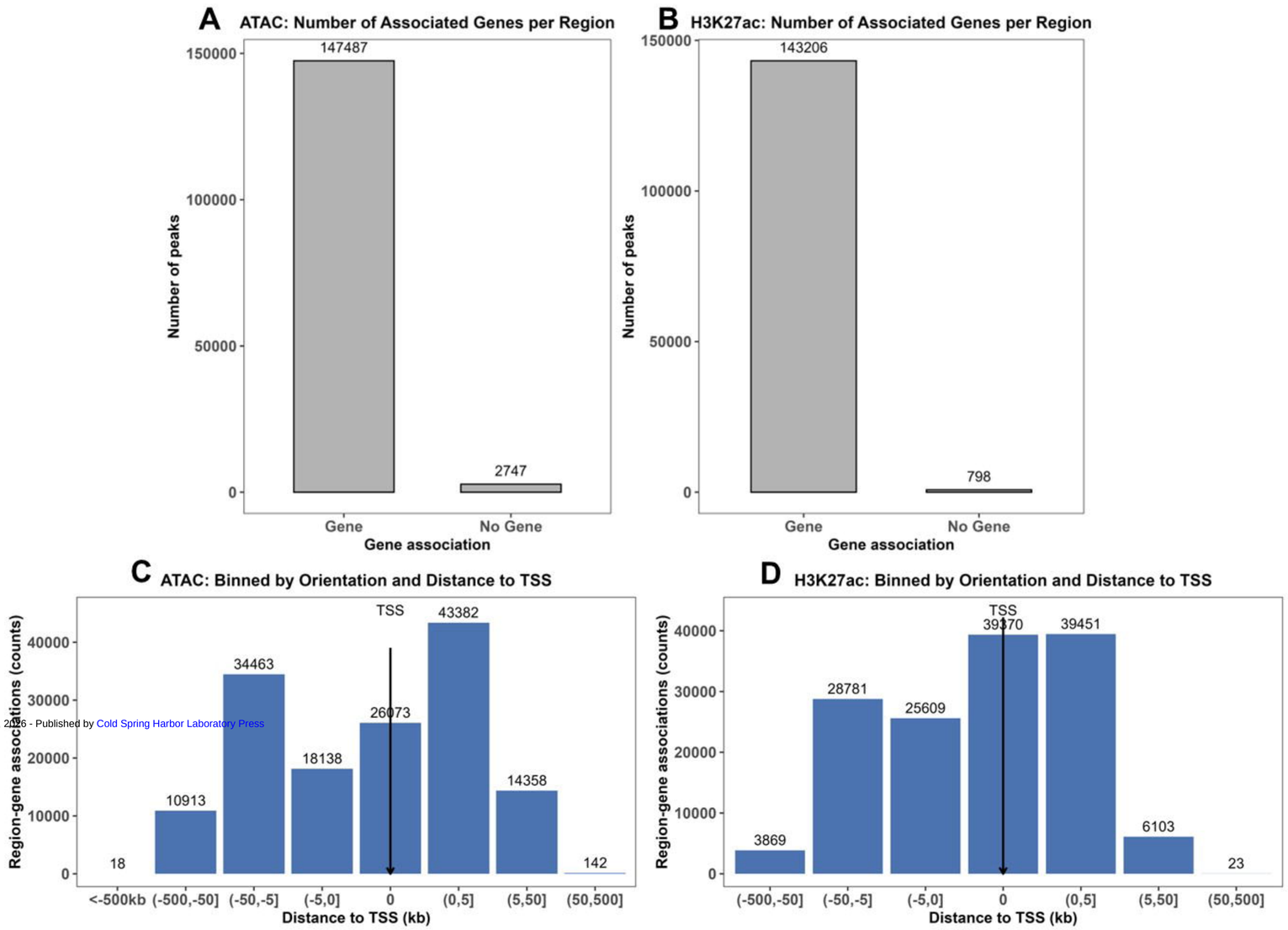

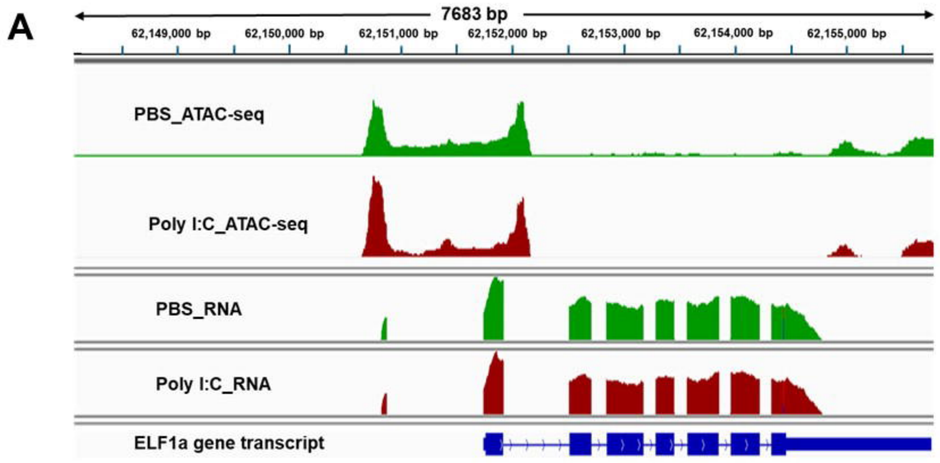

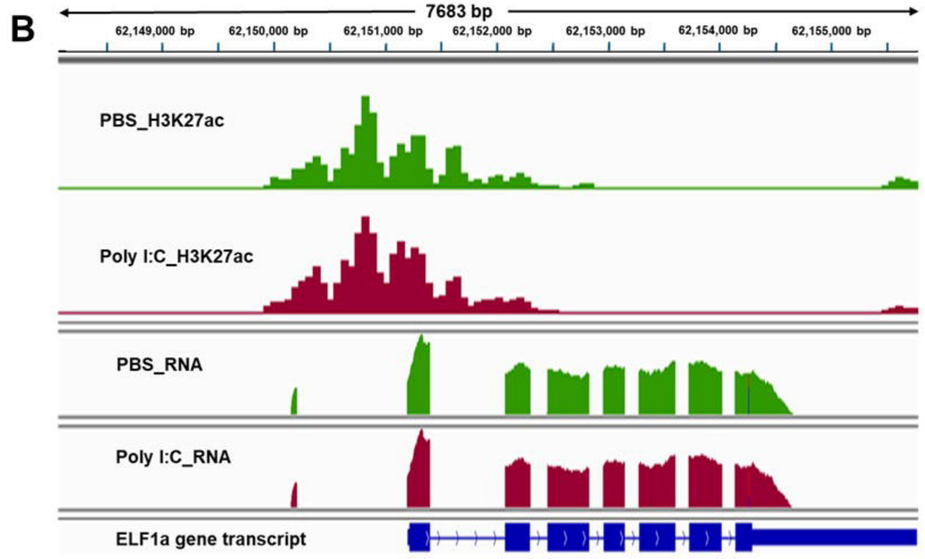

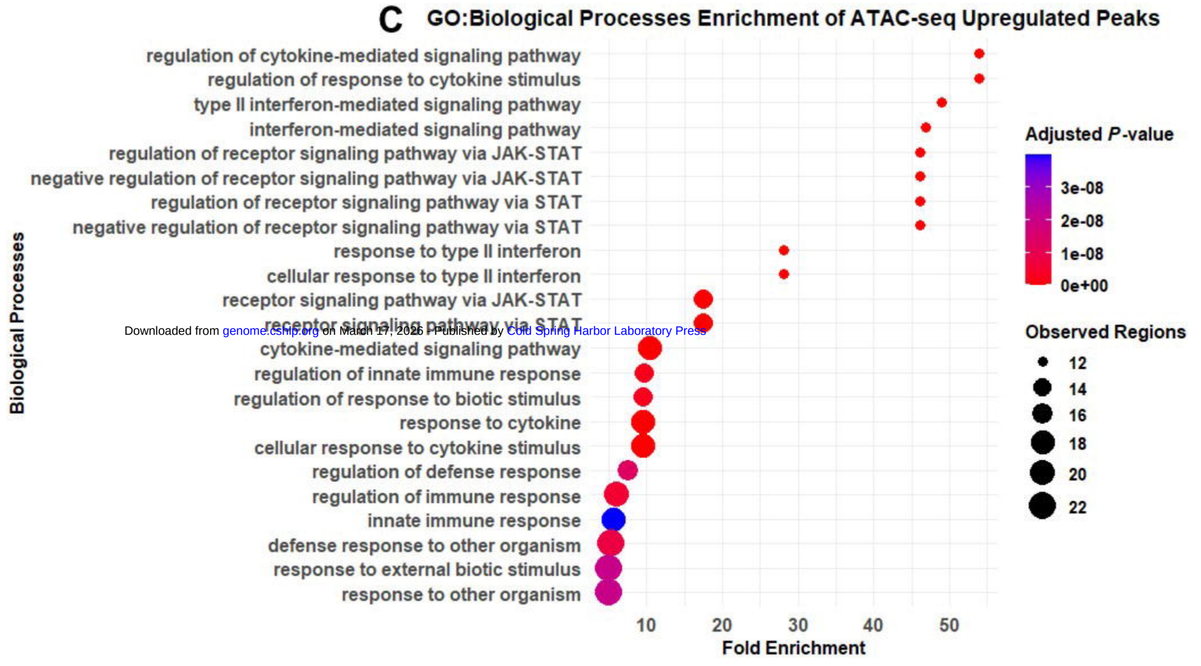

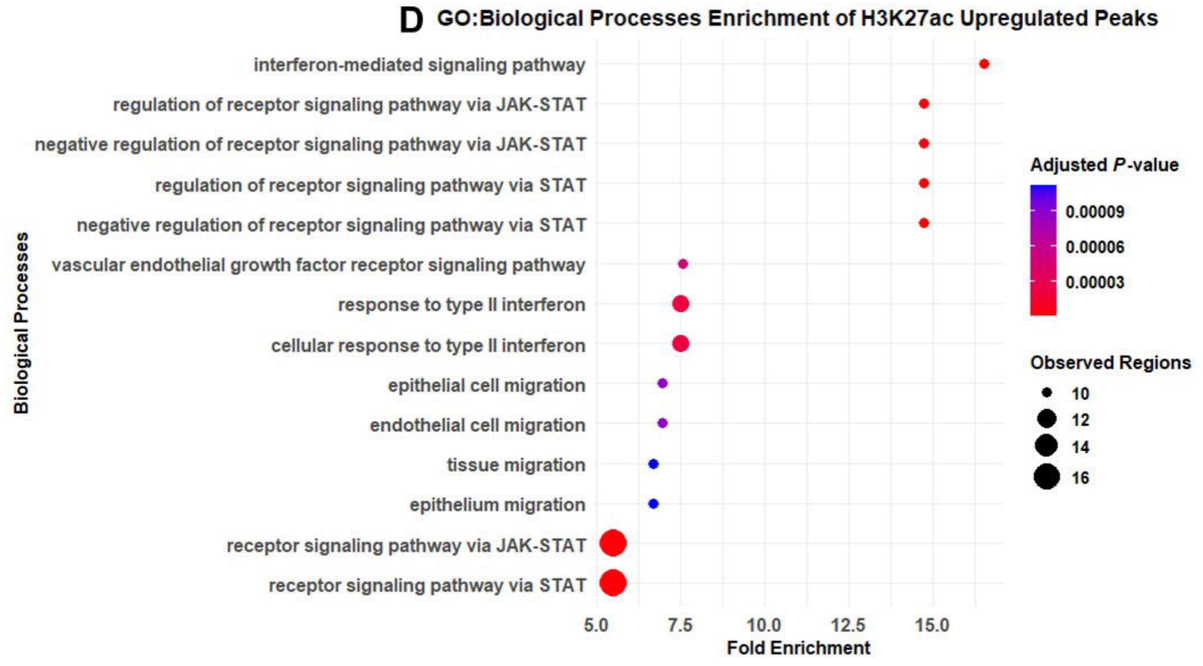

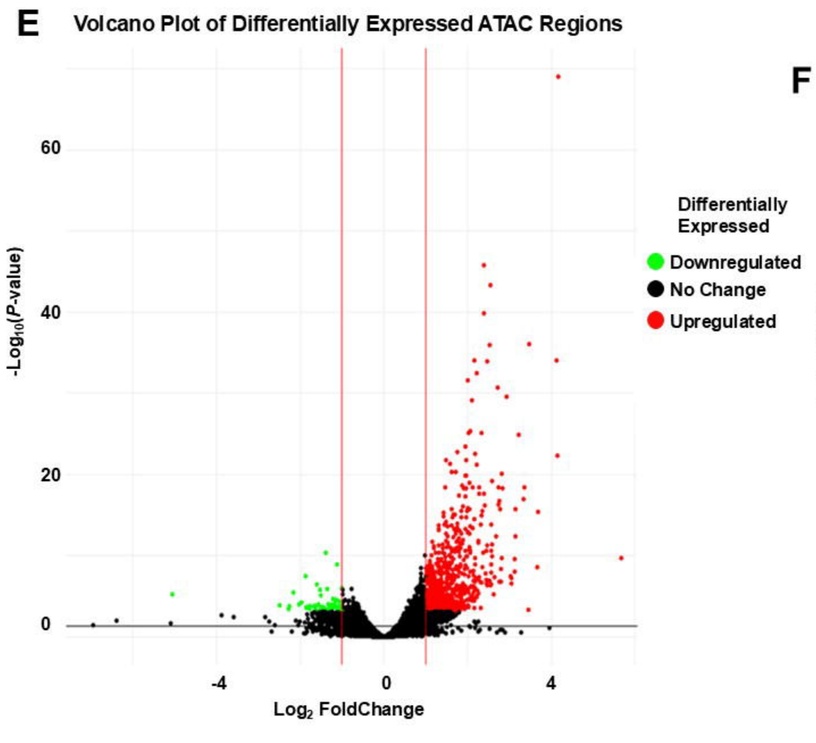

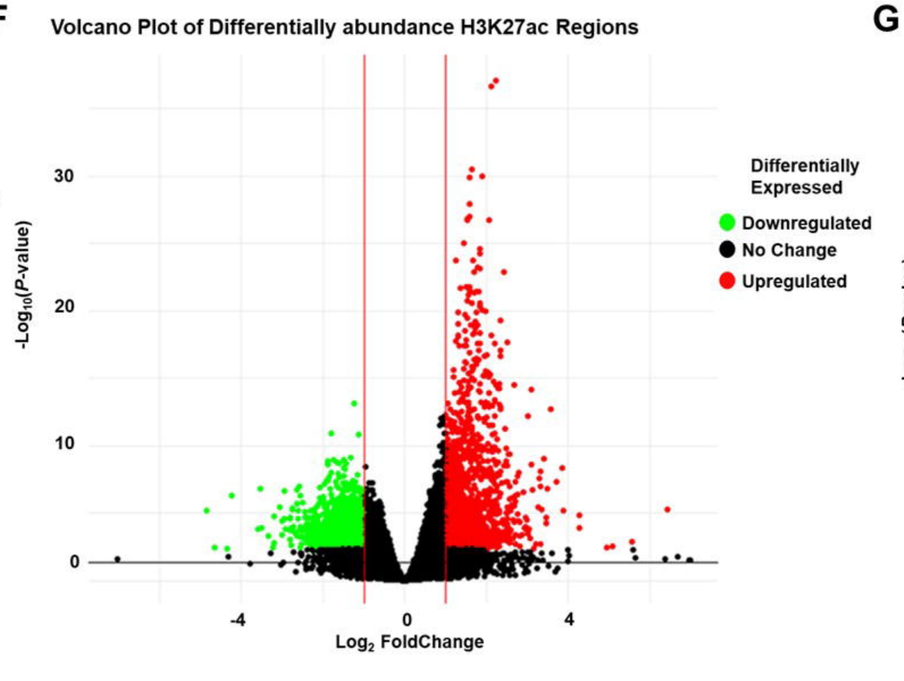

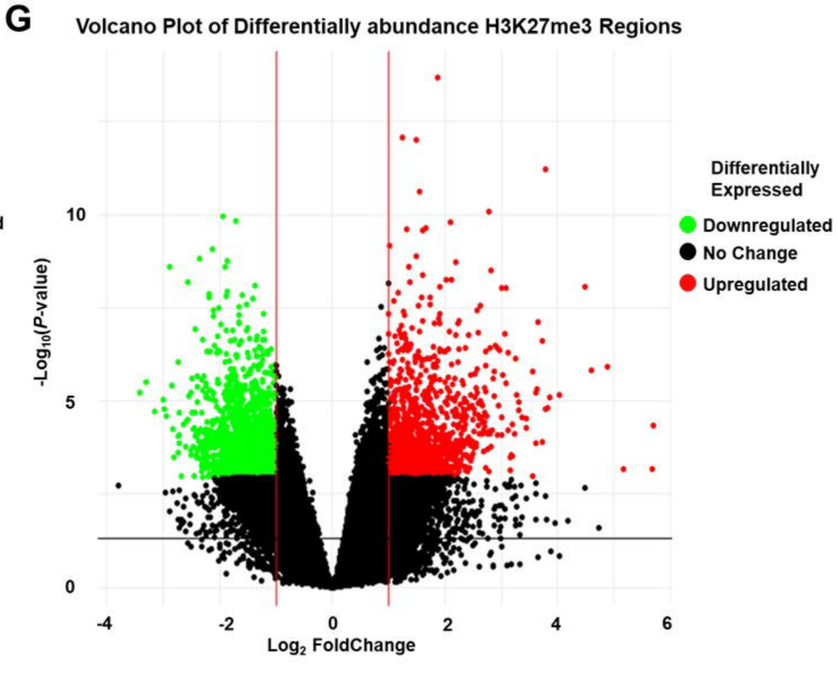

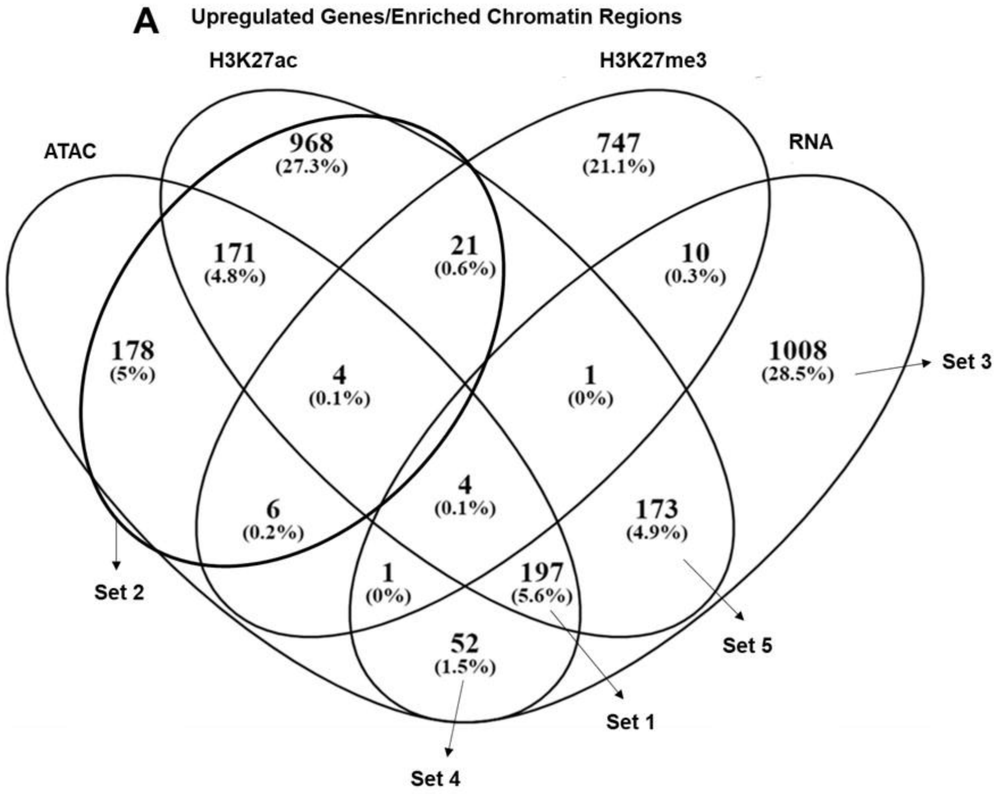

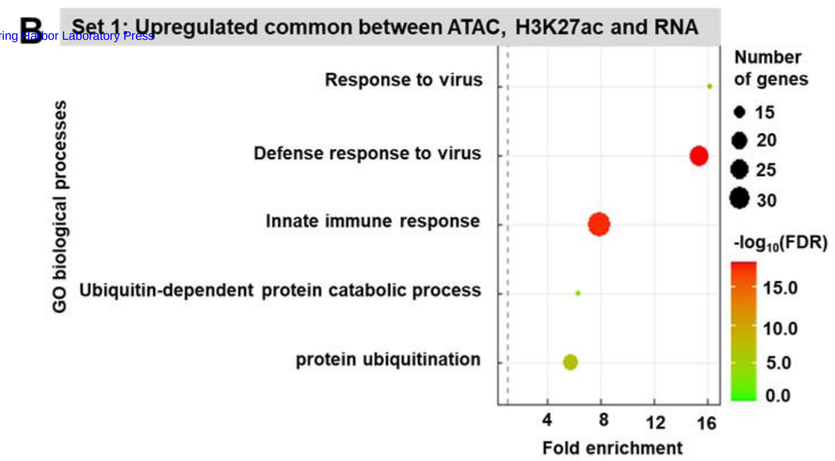

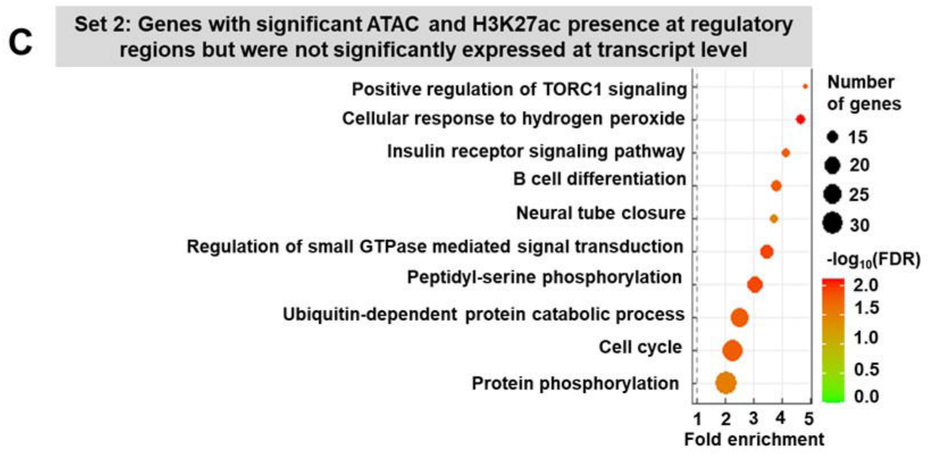

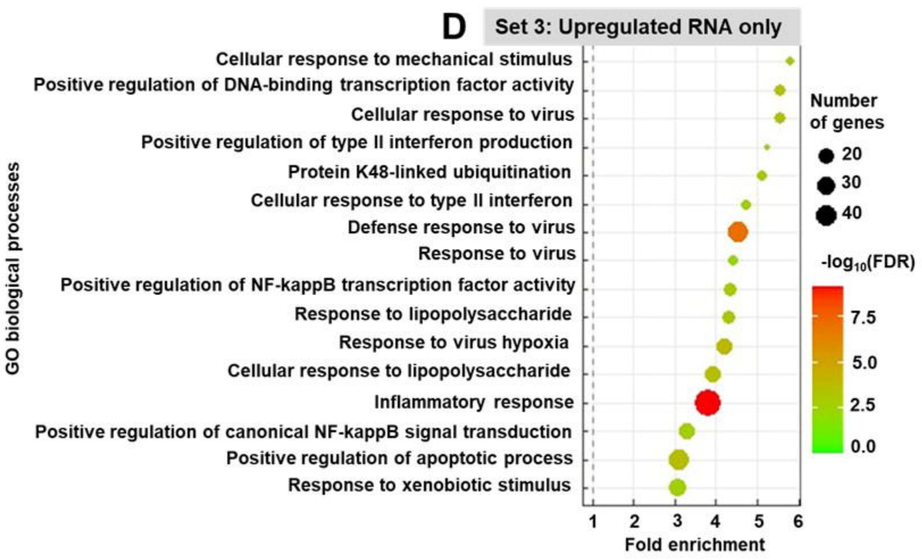

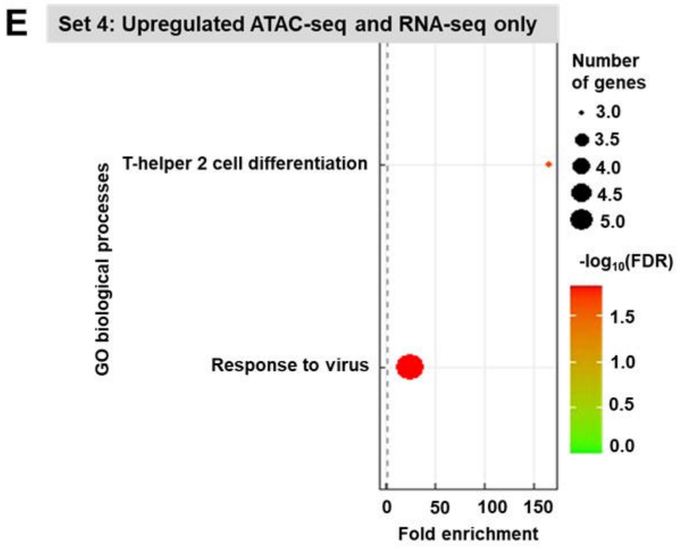

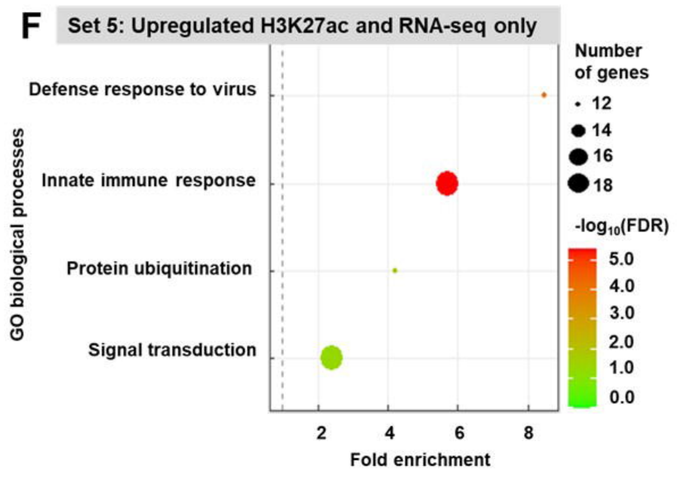

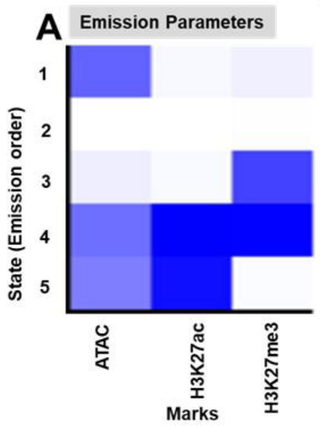

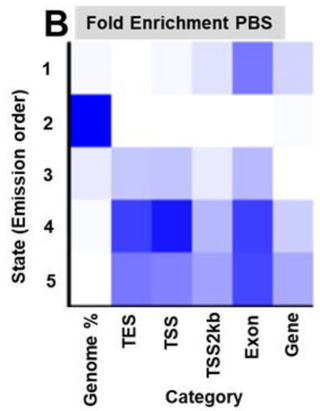

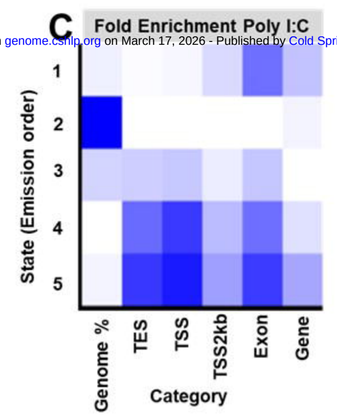

State Annotation

1. ATAC islands
2. Quiescent/Low
3. Repressed state
4. Poised promoter
5. Active enhancers and promoters

D TFBs identified using GimmeMotifs from the enriched regions in state 5, corresponding to active enhancers and promoters

Transcription factors	*Z*-score PBS	*Z*-score polyI:C	% with motif	Logo
STAT6	-2.43	4.56	2	
IRF9	-5.39	4.45	2	
PRDM1	-2.72	3.89	2	
IRF6	-3.18	3.6	2	
JDP2	-4.04	3.39	2	
Nr2e1	-1.99	3.09	<1	
BCL6	-3.25	2.66	<1	
GATA5	3.34	-1.9	2	
ONECUT2	3.56	-2.31	1	
POU1F1	3.32	-2.39	1	
KLF9	3.7	-2.68	2	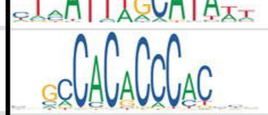
RFX5	3.34	-3.07	3	
TBX19	1.66	-3.08	2	
ZNF93	2.59	-3.17	2	
ZSCAN4	4.09	-3.38	2	
FOXF2	4.15	-4.27	1	

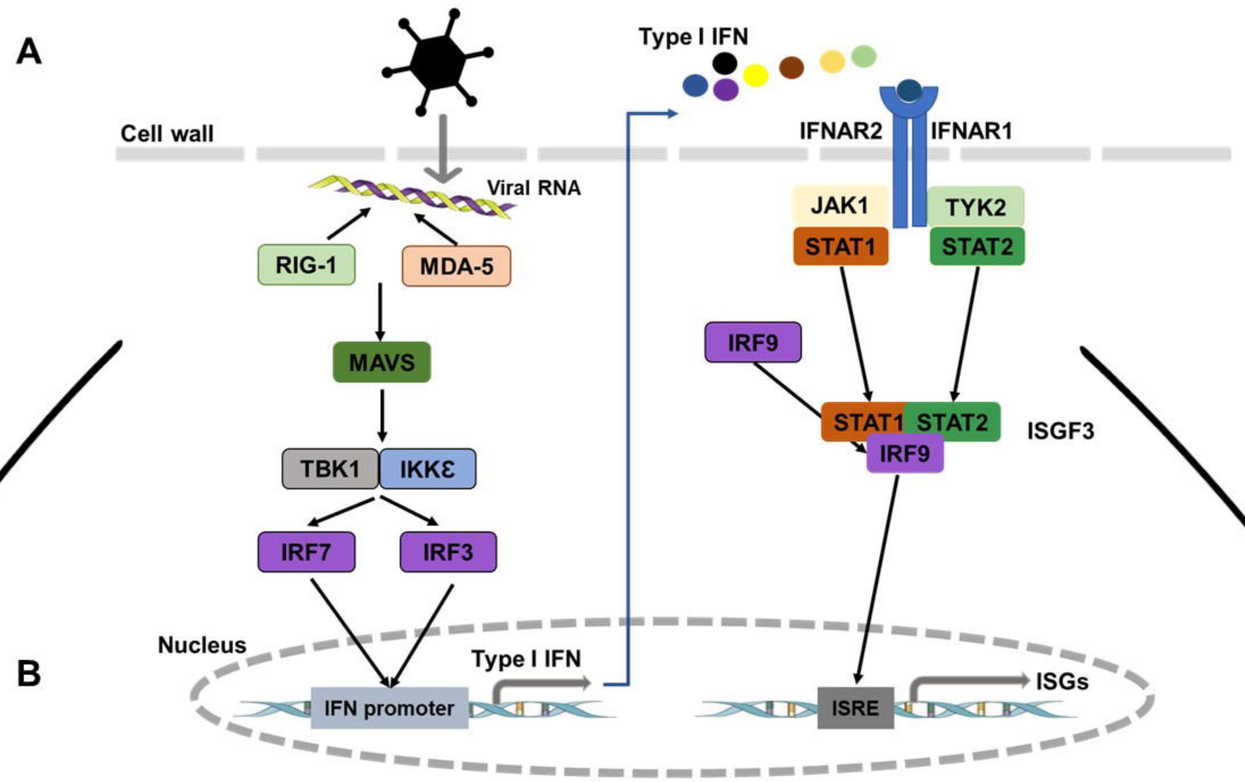

Gene_id	Ensembl_id	ATAC_FC	H3K27ac_FC	H3K27me3_FC	RNA_FC
DHX58(RIG1)	ENSSSAG00000119673	2.78	3.11	-2.43	5.83
IFIH1 (MDA5)	ENSSSAG00000078885	2.80	2.79	-1.62	6.64
IRF3	ENSSSAG00000047292	1.53	3.26	0.00	6.02
IRF7	ENSSSAG00000076373	2.12	3.36	0.00	10.33
STAT1	ENSSSAG00000073567	1.30	2.28	1.16	3.33
STAT2	ENSSSAG00000067332	1.40	2.51	-1.26	3.77
IRF9	ENSSSAG00000080439	1.78	2.53	-1.24	3.70

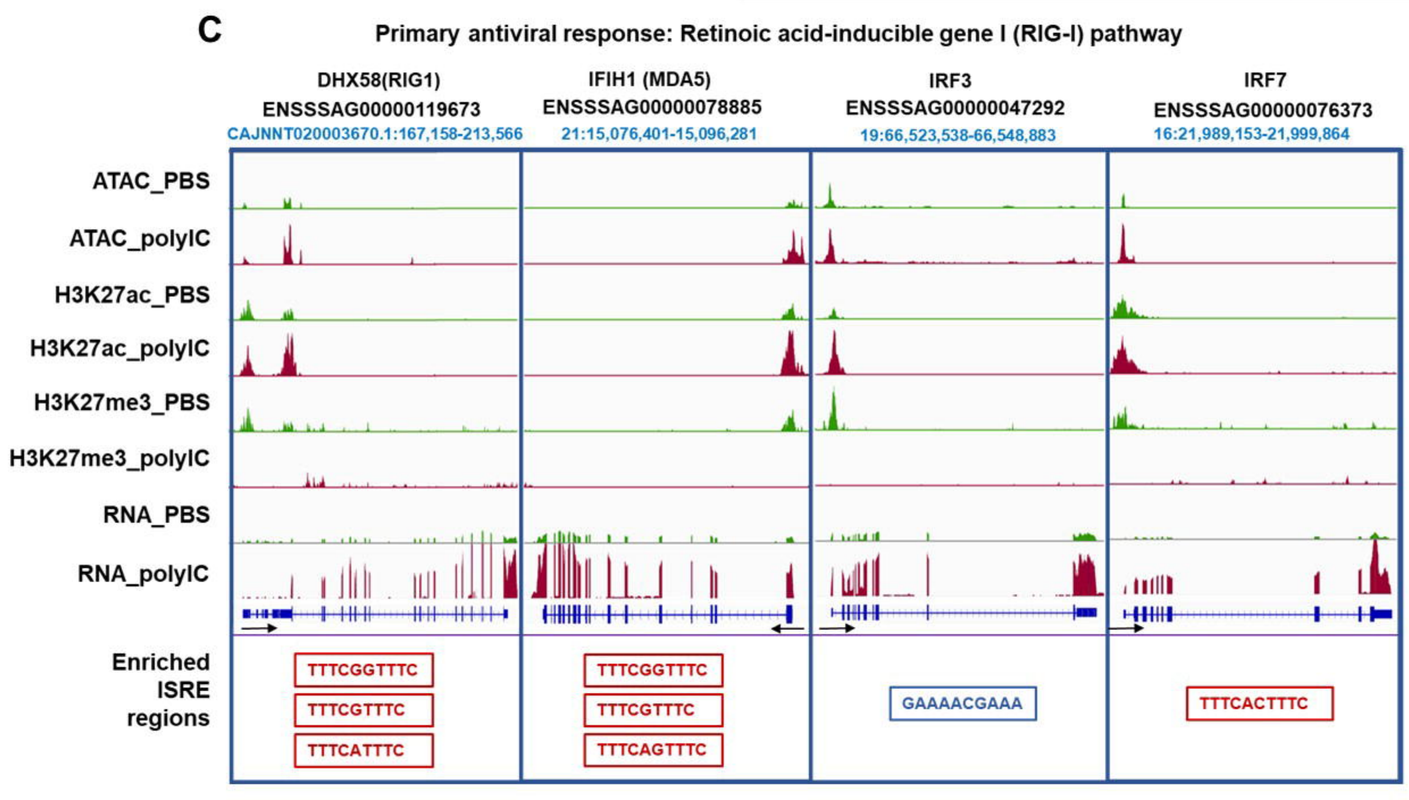

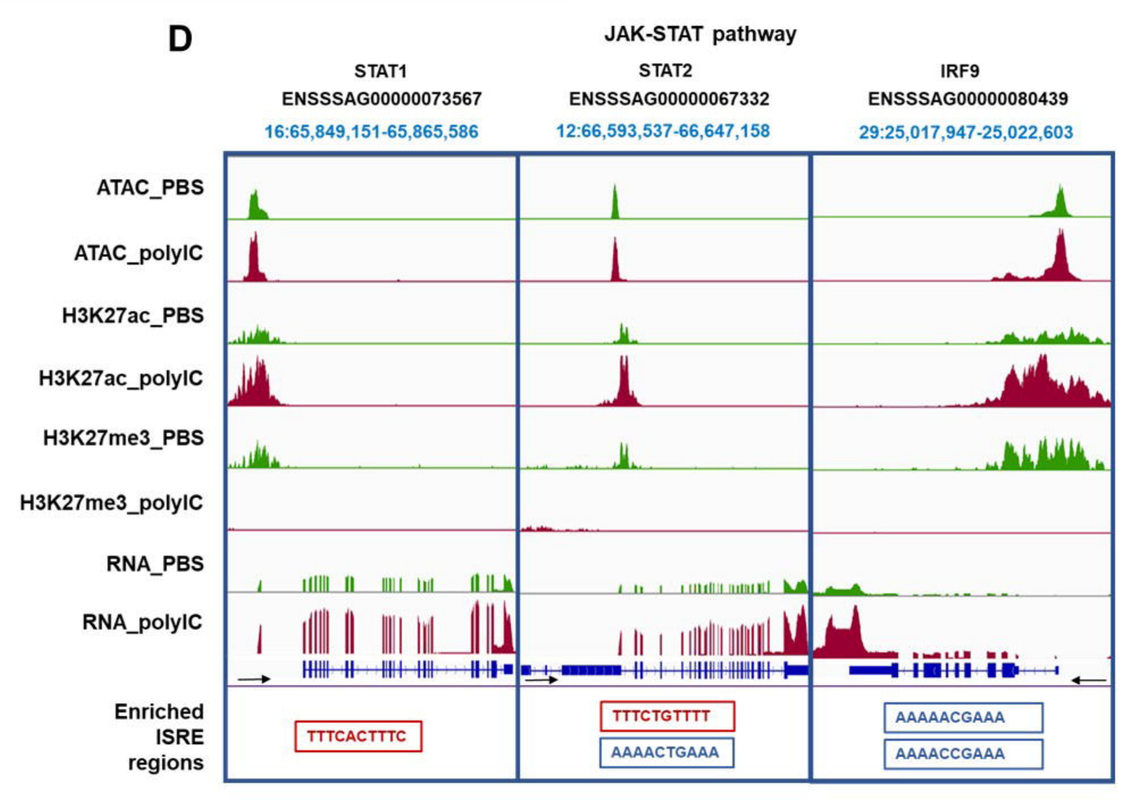

A

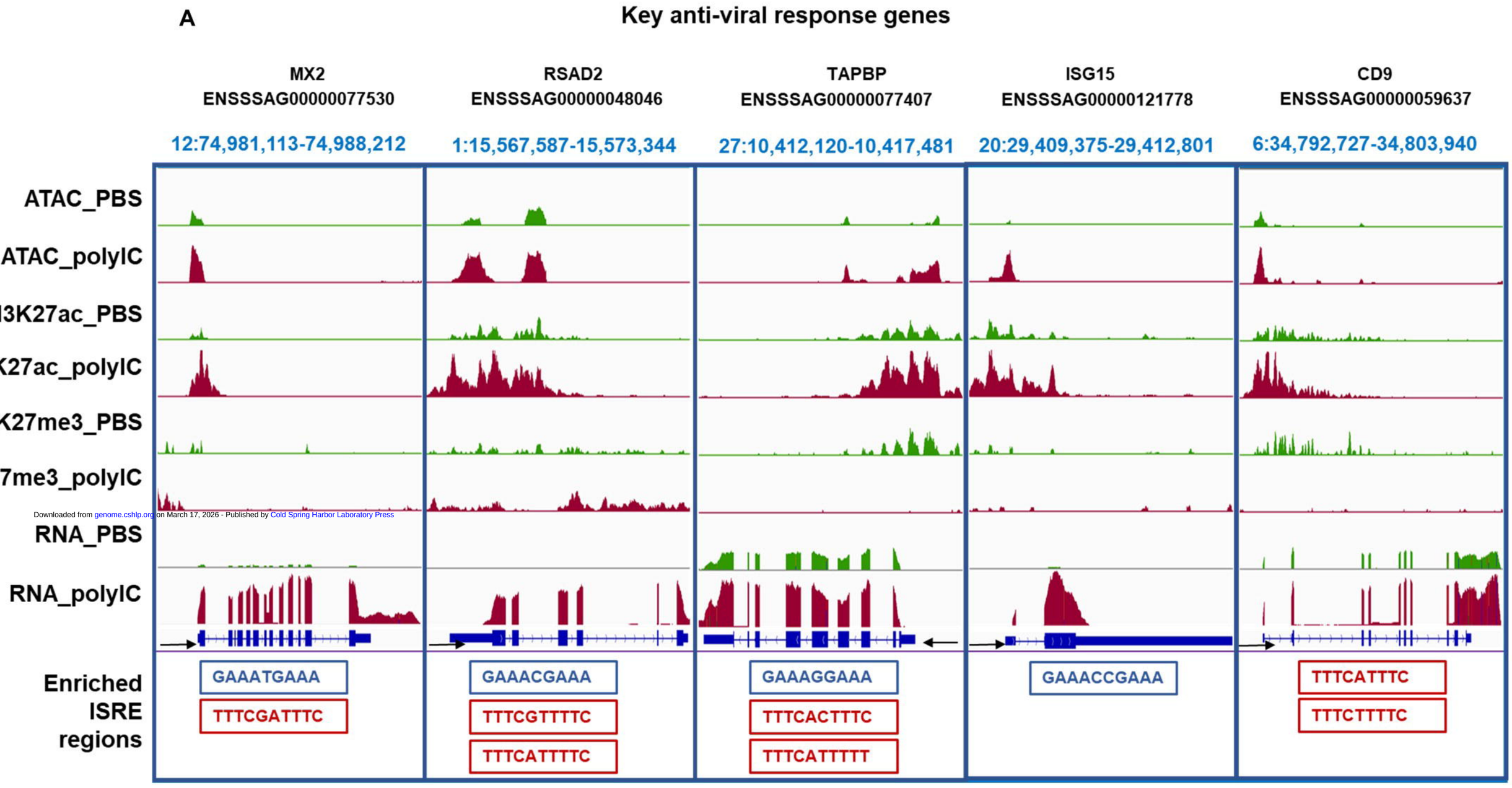

B

Gene_id	Ensembl_id	ATAC_FC	H3K27ac_FC	H3K27me3_FC	RNA_FC
MX2	ENSSSAG00000077530	6.91	4.56	1.77	23.84
RSAD2	ENSSSAG00000048046	2.56	2.62	-2.05	86.03
TAAPBP	ENSSSAG00000077407	2.40	2.38	0.00	2.89
ISG15	ENSSSAG00000121778	4.12	2.17	0.00	44.79
CD9	ENSSSAG00000059637	2.21	2.17	-1.46	3.36

Genomic regulatory landscape underlying the antiviral response of Atlantic salmon

Shahmir Naseer, Thomas C Clark, Bertrand Collet, et al.

Genome Res. published online October 22, 2025
Access the most recent version at doi:10.1101/gr.280579.125